Gesellschaft für Anlagen-
und Reaktorsicherheit
(GRS) mbH

Gas Migration in the Opalinus Clay as a Function of the Gas Injection Pressure

HG-C Project

Final Report

Norbert Jockwer
Klaus Wieczorek

December 2008

Remark:

This report was prepared under the contract No. 02 E 10 226 with the German Bundesministerium für Wirtschaft und Technologie (BMWi). The work was conducted by the Gesellschaft für Anlagen- und Reaktorsicherheit (GRS) mbH.
The authors are responsible for the content of the report.

GRS – 249
ISBN 978-3-939355-24-3

Preface

Beside salt and granite, clay formations are investigated as potential host rocks for disposing radioactive waste. In Switzerland in the canton Jura close to the city of St. Ursanne, an underground laboratory was built in the vicinity of the security gallery of a motorway tunnel. Since 1995, a consortium of 12 international organisations is running this laboratory for investigating the suitability of the Opalinus clay formation with regard to disposal of radioactive waste.

When disposing radioactive waste in clay formations gases like hydrogen, hydro carbons, or carbon dioxide will be generated and released as a result of corrosion of the metallic components of the waste or the containers and by thermal or microbial degradation of organic components within the waste, the backfill or the surrounding clay. These gases are of importance for the long-term safety as they may pressurise sealed areas and be transport medium for volatile radionuclides. In order to quantify the gas migration and the gas pressure evolution it is of importance to know the relevant gas transport mechanisms. Previous tests in the Mt. Terri underground laboratory indicated that gases do migrate into the surrounding clay already at low pressure.

The aim of the HG-C project was to investigate the gas migration into the Opalinus clay in the undisturbed rock outside the excavation damaged zone as a function of the gas injection pressure and to determine the relevant petro-physical parameters of gas advection and gas diffusion.

The project ran from September 2006 to June 2008 and was funded by the German Ministry of Economics and Technology (BMWi) under the contract No. 02 E 10 226.

Table of Contents

1 Introduction

In a nuclear waste repository all the openings such as shafts, galleries, emplacement chambers, and disposal boreholes have to be backfilled and sealed by geotechnical barrier systems to avoid the release of radionuclides into the biosphere above an unacceptable level. The backfill and sealing materials for clay formations may be concrete, clay, and clay-sand-mixtures, depending on the petro-physical conditions of the host rock and the disposal concept. In order to define the requirements for these technical barriers and to ensure long-term safety of the repository, the hydraulic data of the host rock in the vicinity to the artificially generated openings and in the undisturbed areas are essential.

Since about two decades, geological clay formations are investigated with regard to their suitability of hosting a repository for high-level radioactive waste. Underground research laboratories (URL) in clay formations are currently operated or are under construction in the plastic Boom clay formation near Mol in Belgium, the consolidated Callovo-Oxfordian clay formation at Bure in France, and in the consolidated Opalinus clay formation at Mont Terri in Switzerland.

The corrosion of the metallic containers will lead to the release of significant amounts of hydrogen /RÜB 04/ /RÜB 05/ after the closure of the disposal areas, healing of the excavation damaged zone (EDZ), and re-saturation of the host rock and the backfill. Additionally, carbon dioxide will be generated and released as a result of oxidation or thermal degradation of the organic material contained in the clay /JOC 06/. These gases may lead to the development of elevated gas pressures in the repository which could lead to fracturing of the host rock if the gas pressure exceeded the minimum principal stress (σ_3) in the rock. The integrity of the host formation would be impaired and the release of radioactive material from the disposal rooms might be possible.

The gas pressure build-up in a repository is controlled by the gas production rate as well as by the gas transport properties of both the host rock and the engineered barriers.

Important gas transport mechanisms are diffusive flow in the non water saturated and in the water saturated pores (diffusion in the gas and in the liquid phase), advective gas flow (two-phase flow) in the non water saturated pores, and, at pressures near to or exceeding the minimum principal stress, dilatancy controlled advective flow and

advective fracture flow. These processes are controlled by the gas pressure and the pore water pressure. At low gas generation rates, it is expected that all gas can be transported by diffusion, advection and two phase flow through the host rock. Fracturing will only occur in case of high gas production rates.

In the HG-C project the gas migration in the Opalinus clay as a function of the gas pressure in the range between 0.1 MPa (atmospheric pressure) and about 4.0 MPa (gas frac pressure) was investigated. This report presents the results.

2 Issues and Objectives

Different mechanisms for gas migration in clay formation are feasible:

- Dissolution of the gases in the pore water and diffusion of these gases in the liquid phase.

- Advective and diffusive gas transport in the gas phase if the host rock is not completely water saturated as a result of drying or gas storage in sand and calcite layers.

- Two-phase gas-water flow in the pore volume of the host rock if the gas pressure exceeds the capillary pressure. In the Opalinus clay at Mt. Terri gas entry pressure were determined at 2 MPa - much below the least principal stress /NAG 02-1/, /NAG 02-2/.

- Gas flow on micro-fracs if the gas pressure exceeds the least principal stress and micro-fracs are generated. The investigation at the HE-D test indicated that this can happen at a gas pressure above 2.5 MPa /ZHA 07/.

- Gas flow on macro-fracs if the gas pressure exceeds the least principal stress and the gas generation rate is so high that the gases cannot be drained off through the micro-fracs.

The gas migration in the Opalinus clay of Benken and Mt. Terri was already observed below the least principal stress (σ_3) in the rock /RÜB 04/, /NOS 05/. The mechanism of this gas migration was neither investigated in the laboratory nor in-situ /NEA 04/. It was assumed that within the clay formation dilatancy controlled micro-fracs are generated through which the gases are migrating into the surrounding host rock. This assumption has to be proven by further investigations.

In previous tests at the Mont Terri Rock Laboratory (MTRL) significant gas migration in the Opalinus clay was observed outside the EDZ already at pressures much below the water formation pressure. In the HE-B test hydro carbons and carbon dioxide were released from the host rock as a result of heating. In the gastight sealed observation boreholes only low pressure increases up to 0.2 bars were observed, whereas the concentration of carbon dioxide increased up to 20 vol% /JOC 06/. This result indicates

that even at low gas pressure gas is migrating into the undisturbed surrounding host rock. In the HE-D test gas injections were performed into gastight sealed intervals outside the EDZ. Significant gas migration was observed already at pressures below 1.5 MPa. The water formation pressure was in the range of 2.0 to 3.0 MPa. Gas fracs were generated at a pressure above 3.5 MPa /ZHA 07/.

As a consequence, several complementary tests which investigate the gas migration inside and outside the excavated disturbed zone (EDZ) were started at the MTRL in recent years:

- In the **HG-A** experiment NAGRA investigates in a horizontal borehole of 1,0 m diameter and a length of 10 m both the development of the EDZ with the time and the gas migration in that zone. At the front end this borehole was sealed with a special packer system and the residual volume of the borehole at the back end was backfilled. For the investigation of the gas migration the pore volume of that backfill is inflated with gas and at different gas pressures the gas flow is recorded for holding that pressure constant. Additionally in the surrounding host rock the drying, re-saturation, and the deformation is determined.

- In the **HG-B** experiment BGR investigates the extension and the anisotropy of the EDZ around galleries of different ages. In sealed boreholes up to 20 m depth the gas flow at different constant pressure are determined. With special surface packers the gas flow at the gallery walls are investigated.

- In the **HG-C** experiment which is subject of this report the diffusive and advective gas migration outside the EDZ between atmospheric and gas entry pressure, but below the gas frac pressure were investigated. This investigation was performed in inclined boreholes with a length of 10 m drilled parallel and perpendicular to the bedding.

- In the **BET** experiment GRS investigates outside the EDZ the generation of gas fracs at pressure above 3.5 MPa, the advective gas flow in these fracs and the healing of the fracs when reducing the gas pressure. These investigations are also performed in inclined boreholes with a length of 10 m drilled parallel and perpendicular to the bedding. In the Mont Terri laboratory, HG-C and BET run together under the title of HG-C.

The objectives of the HG-C (in the narrow sense) were to

- Investigate which gas migration mechanisms are relevant at different gas pressure levels, especially below the minimum principal stress, by injecting a defined tracer gas mixture (2 vol% H_2, He, Ne, Kr, C_4H_{10}, and SF_6 in 88 vol% N_2) into sealed boreholes in the rock and monitor the concentration/pressure changes. The tracer gases were chosen because of the difference in their molecular mass, solubility in water, and sorption behaviour.

- Quantify migration of the different tracer gases, in terms of determination of diffusion coefficients or effective permeability.

- Determine gas entry pressures and effective permeabilities at elevated pressure near or above the minimum principal stress.

3 Test Field Description

3.1 Location and Geology

The Mont Terri Rock Laboratory (MTRL) has been excavated parallel to the security gallery of the Mont Terri motorway tunnel in the north-western part of Switzerland on the south-western slope of the Mont Terri anticline (Fig. 3.1). It is located in the Opalinus clay formation consisting of three main facies: the sandy facies, the shaly facies, and the sandy carbonate-rich facies. More details about the different lithologies can be found in /THU 99/. The bedding planes plunge towards the south-east with an azimuth of 140 – 150°. The apparent thickness of the Opalinus clay is about 160 m. Its current overlay varies between 250 and 320 m, while it is estimated to have reached at least 1000 m in the past. The pores in the clay rock are saturated with water, but water circulations are practically negligible due to its very low permeability and pressure gradient. In the far regions from the openings in the MTRL the pore-water pressure amounts to about 2.1 MPa and the rock temperature is about 15 °C.

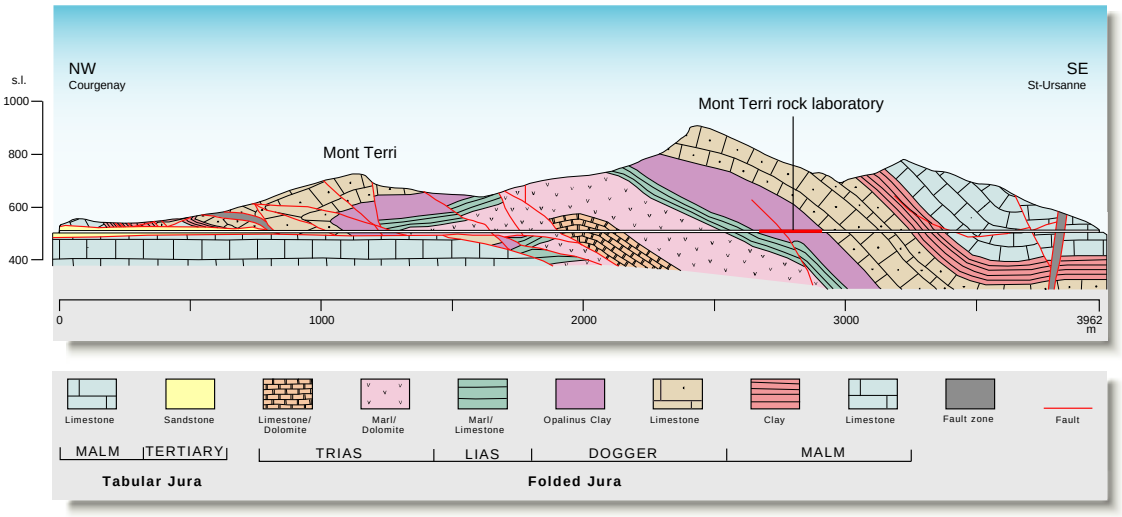

Fig. 3.1 Geological profile along the motorway tunnel showing the location of the Mont Terri Rock Laboratory

The state of stress at the MTRL is estimated according to /BOS 03/:

- the maximum principal stress σ_1 with a magnitude range of 6 – 7 MPa and a sub-vertical direction of 210° azimuth and 70° dip,
- the intermediate principal stress σ_2 with a magnitude range of 4 – 5 MPa and a sub-horizontal direction of 320° azimuth and 10° dip (sub-parallel to the motorway tunnel and the security gallery), and
- the minimum principal stress σ_3 with a magnitude range of 2 – 3 MPa and a sub-horizontal direction of 50° azimuth and 20° dip (more or less normal to the motorway tunnel and the security gallery).

The HG-C was performed in the SB niche (Fig. 3.2) located in the clay-rich shaly facies near the main gallery Ga04. It was built in 2004 for testing the gas and water permeability of different clay-sand mixtures as potential sealing materials in the dry and wet stage. For these tests four vertical boreholes with a diameter of 30 cm and a depth of 3 m were drilled into the floor of this niche.

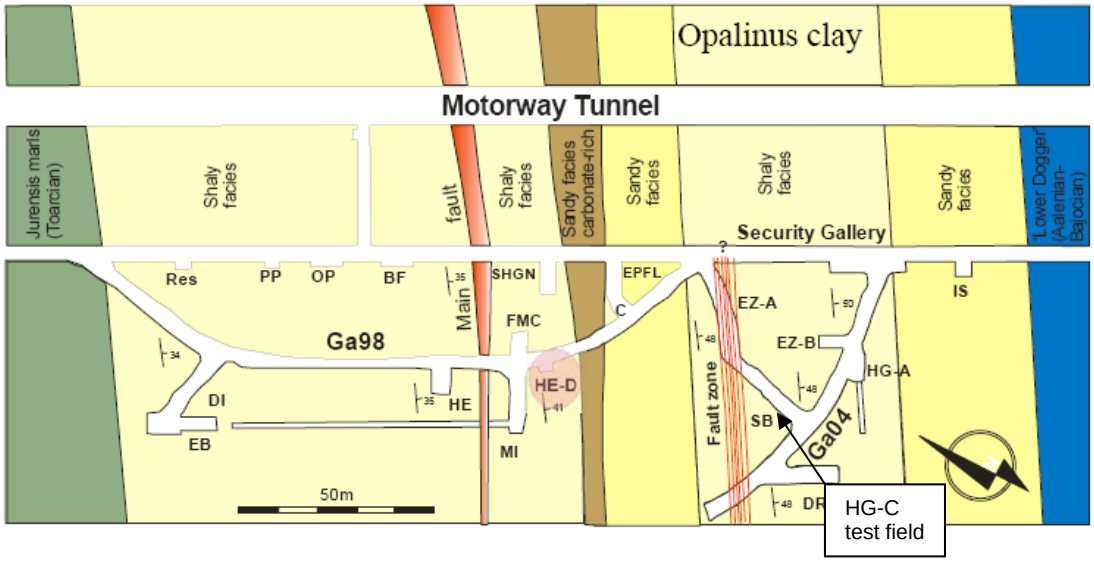

Fig. 3.2 Plan view of the Mont Terri Rock Laboratory showing the location of the SB niche with the HG-C test field

For the investigations of the HG-C project six boreholes with a diameter of 76 mm and a length of 10 m were drilled into the wall of the niche as shown in Fig. 3.3, three of them (BHG-C1, BHG-C2, BHG-C3) at the south-east wall with a dip of 40° parallel to the bedding and three (BHG-C4, BHG-C5, BHG-C6) at the north-west wall also with a

dip of 40°, but perpendicular to the bedding. The boreholes BHG-C1 and BHG-C4 were used for gas injection. Boreholes BHG-C2 and BHG-C5 have a horizontal distance of 50 cm to the injection boreholes and boreholes BHG-C3 and BHG-C6 have a vertical distance of 50 cm to the corresponding injection borehole. All the boreholes were drilled by GRS staff with a Longyear drill rig, three bits rotary drilling crown, and drilling rod for flushing with air.

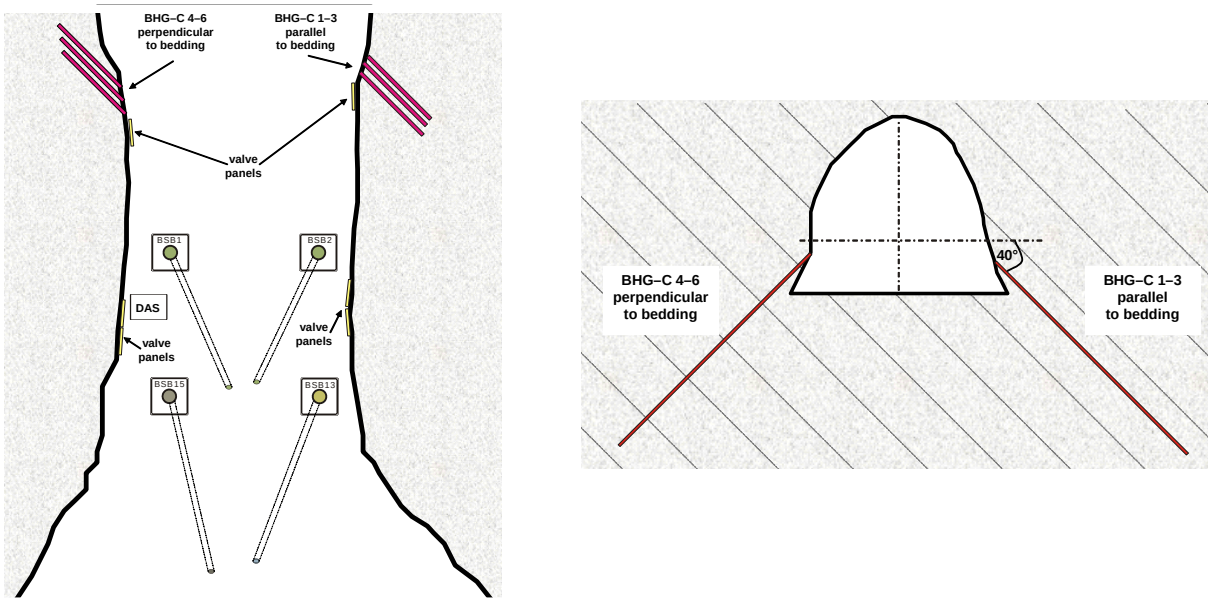

Fig. 3.3 Plan view and cross section of the SB niche with the HG-C boreholes perpendicular and parallel to the bedding

3.2 Instrumentation of the Test Field

Right after drilling the directions of all boreholes were measured over the whole length by a survey office. With the results the distances with depth between the boreholes could be calculated.

As drilling was performed by flushing with air the host rock in the near vicinity of the borehole may have been dried. In order to re-saturate the host rock 2 litre of Pearson water (artificial pore water) were filled into each borehole via a hose which was injected to the back end of the borehole and withdrawn afterwards.

All six boreholes were sealed with quadruple packer systems for gas testing in separate intervals. The packer systems were manufactured by the Swiss company SOLEXPERTS AG. The packers consist of a 50 mm stainless steel tube to which four

inflatable rubber seals are mounted. From each seal element a capillary runs to a valve panel in the niche for inflation with water up to a pressure of 4.0 MPa. Between the rubber seals sintered stainless steel tubes with a porosity of 50 vol% were installed in order to have a central sample interval and two additional guard intervals which withstand the convergence pressure of the surrounding host rock. The sintered stainless steel tubes also guarantee a defined volume. From the front end and the back end of each interval capillaries run to the niche. All capillaries were connected to valve panels mounted to the niche wall. For observation and recording of the water pressure in the sealing elements and the gas pressure in the intervals, the panels were equipped with optical and electronic pressure gauges which were connected to the data acquisition system.

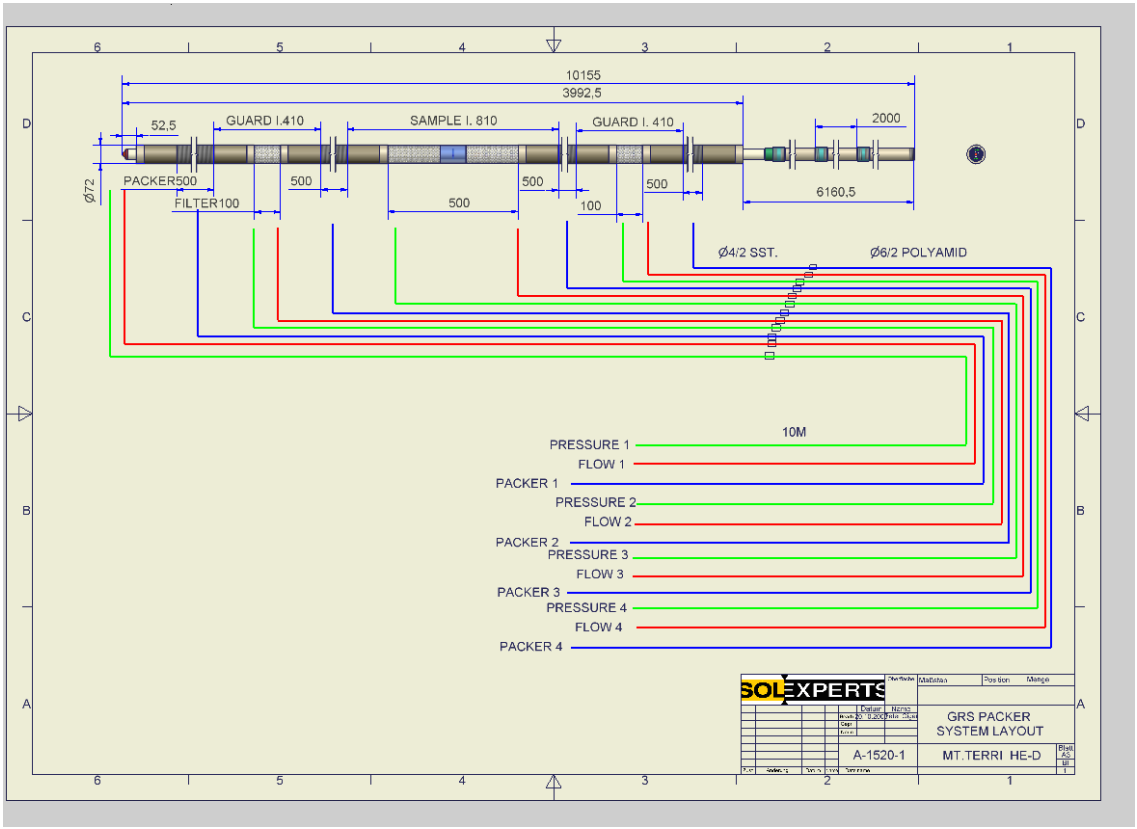

Fig. 3.4 Principle drawing of a quadruple packer system with the capillaries for inflation, gas injection, and pressure determination

A principle drawing of the packer system with the capillaries for inflation of the sealing elements (Packer 1 to 4), for gas injection (FLOW 1 to FLOW 4), and for pressure measurement (PRESSURE 1 to PRESSURE 4) is shown in Fig. 3.4, and Fig. 3.5 shows the boreholes BHG-C1 to BHG-C3 with the valve panels at the niche wall.

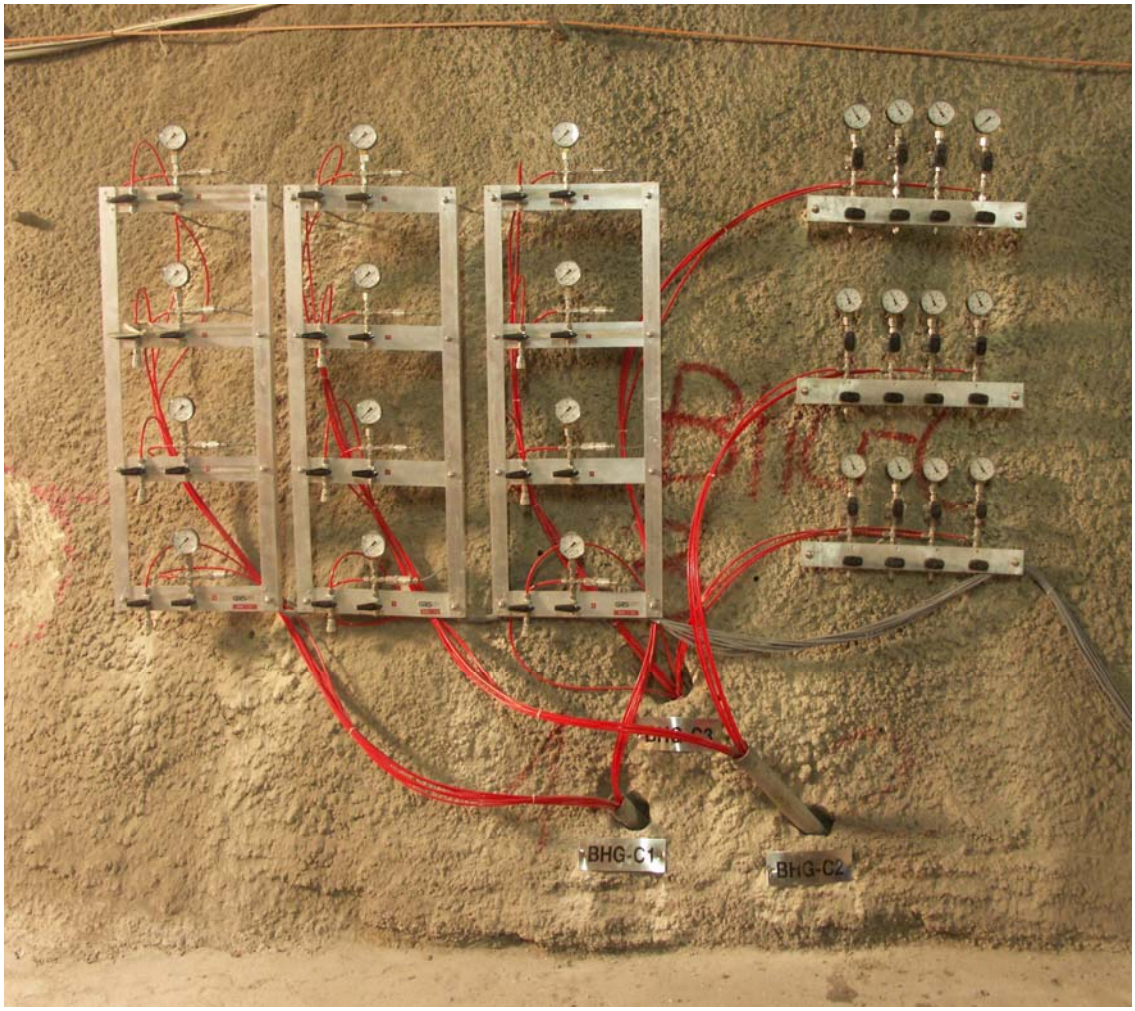

Fig. 3.5 Boreholes BHG-C 1, BHG-C2, and BHG-C3 and the valve panels with the pressure gauges (right: packer inflation; left: gas injection and gas sampling)

The packers were injected into such depth that at the back end of the boreholes a residual volume with a length of 10 cm remained and that the respective test intervals of each packer were in the same plain perpendicular to the boreholes. The water which was filled into the boreholes was displaced by the packer. It filled all the test intervals and the residual borehole volumes above the packers.

After installation of the packers in the boreholes and after connecting the capillaries to the corresponding valves, all the packers were inflated to 40 bar with water using a manual pump. For the extraction of the air in the injection tube and in the dead volume of the packer the system was evacuated via one valve and capillary, via the other valve and capillary it was filled with water and inflated to 4.0 MPa. One day later the pressure had decreased by about 1 MPa. All packers were again inflated to 4.0 MPa.

One month after inflation the pressure was checked again. It had decreased to a level of 2.5 to 3.0 MPa in all the packers. All packers were again inflated to 4.0 MPa. After two further inflations within the next two months the pressure remained constant at about 4.0 MPa. Afterwards all the test and guard intervals of the packer systems were purged with pure nitrogen and the Pearson water in these intervals was displaced by nitrogen. The residual volumes at the deep end of the boreholes in front of the packer systems remained filled with water for the determination of the pore water pressure in the surrounding host rock.

In addition to the borehole instrumentation, two precision balances were available to measure gas mass during the gas injection tests.

3.3 Data Acquisition

The pressure and balance data in the HG-C project (and also in the SB and BET projects) were collected and processed by use of a GeoMonitor system of Solexperts AG. The system was already running for two years before the measurements of the HG-C project started. The principle layout of the system is shown in Fig. 3.6.

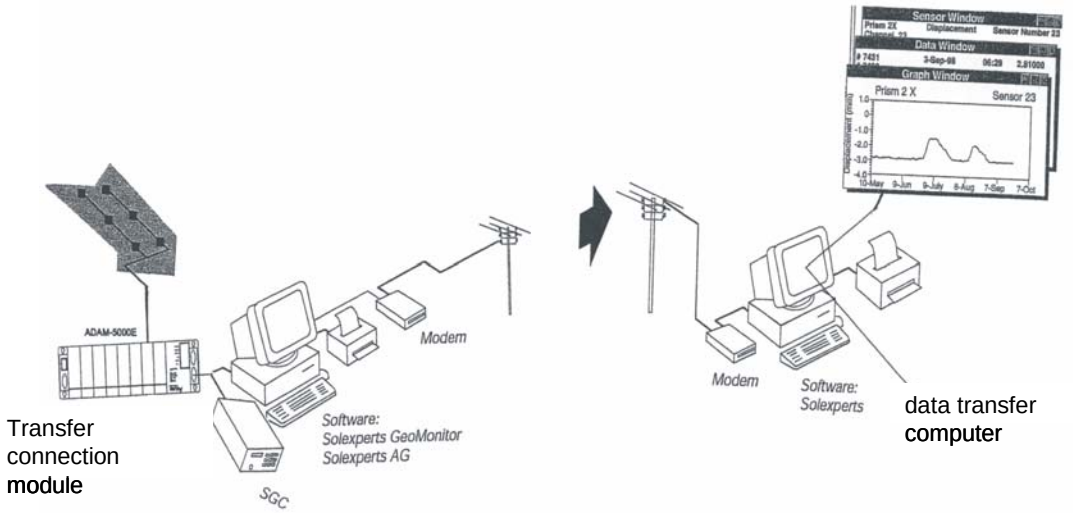

Fig. 3.6 Principle layout of the Data Acquisition System (DAS)

The data acquisition system (DAS) is mounted in a 19 inch rack. It is designed for up to 100 measuring channels (80 analogue and 20 digital channels) and consists of the following components:

- Computer
- GeoMonitor Controller (SGC) with WatchDog
- Data transmission and control system ADAM 5000
- Inputs for analogue measuring sensors
- Interface for balances (digital measuring sensors)
- Modem for data transmission

The following types of transducers were scanned by the system:

- Pressure transducers, absolute pressure 0-20/0-30/0-50 bar, 4-20 mA
- Flow meters, 0-50/10-500/100-5000 ml/min, 4-20 mA
- Digital balances, 0-15 kg
- Resistance temperature sensors Pt 100

The monitoring software developed by SOLEXPERTS runs under Windows and controls:

- Data acquisition (scanning rate etc.)
- Display of measuring results
- Configuration and control of measuring ranges
- Automatic alarm in case of limit accidence
- Automatic reporting and monitoring of measuring activities

Furthermore, data transmission software is implemented in the system. Fig. 3.7 shows the system as compiled before start-up of the tests.

Fig. 3.7 Data acquisition system – front view (left) and rear view (right)

4 Methods of Investigation

Gas migration in porous media depends on the petrophysical parameters porosity, diffusivity, and permeability, but also on the solution of the gases in the aqueous phase and on the physico-chemical interaction of the gases with the internal surfaces of the different media. The solubility to water may be of importance as Opalinus clay contains in the range of 18 weight% pore water. In order to determine these effects, tracer gases with different solubilities to water, different sorption behaviours, and different molecular weights as listed in Tab. 4.1 were used for the investigations of the migration in the Opalinus clay. As the diffusivity in air and water is proportional to the factor $\frac{1}{\sqrt{M}}$ /JOS 72/ (M = molecular weight), this factor is also displayed in the table.

Tab. 4.1 Tracer gases with their physical parameters relevant for gas migration

Tracer gas	Molecular weight [M]	$\frac{1}{\sqrt{M}}$	Diffusivity in air [m^2s^{-1}]•10^{-4}	Diffusivity in water [m^2s^{-1}]10^{-9}	Solubility in water (1 bar) [l gas kg^{-1} water]
Hydrogen	2.0	0.70	0.700	3.81	0.0176
Helium	4.0	0.50	0.698	5.8	0.0083
Neon	20.0	0.22	*0.307*	2.8	0.01
Iso-butane	56.1	0.13	*0.154*	*1.154*	0.0325
Krypton	83.8	0.11	0.149	*1.276*	0.59
Sulphur hexafluoride	146.0	0.08	0.075	*0.928*	0.0056
Nitrogen	28.0	0.19		2.34	0.0156

Values are from literature /LID 94/, /DAN 92/
Italic values are calculated

For investigating the gas migration as a function of the gas pressure three methods were used:

1. Purging an interval with the tracer gas mixture at atmospheric pressure, sealing it for a defined time period and determining the tracer gas concentration decrease after that time period.

2. Pressurizing an interval with the tracer gas mixture to a defined pressure step, sealing it afterwards and determining the pressure and concentration decrease with time.

3. Pressurizing an interval with nitrogen to a defined pressure step, holding that pressure constant and determining the gas flow for holding that pressure constant (constant head test), and recording the pressure decay after stopping the gas flow.

With the results of these investigations and available computer codes the parameters of gas migration as diffusivity and permeability were derived.

The following nomenclature was used for the test intervals of each borehole:

- deep end of the borehole: Interval 1
- guard interval at the back end of the packer: Interval 2
- sample interval at the centre of the packer: Interval 3
- guard interval at the front end of the packer: Interval 4

The Figs. 4.1 and 4.2 show the cross and longitudinal sections of the two test areas:

- Boreholes BHG-C1, BHG-C2, and BHG-C3 drilled parallel to the bedding
- Boreholes BHG-C4, BHG-C5, and BHG-C6 drilled perpendicular to the bedding

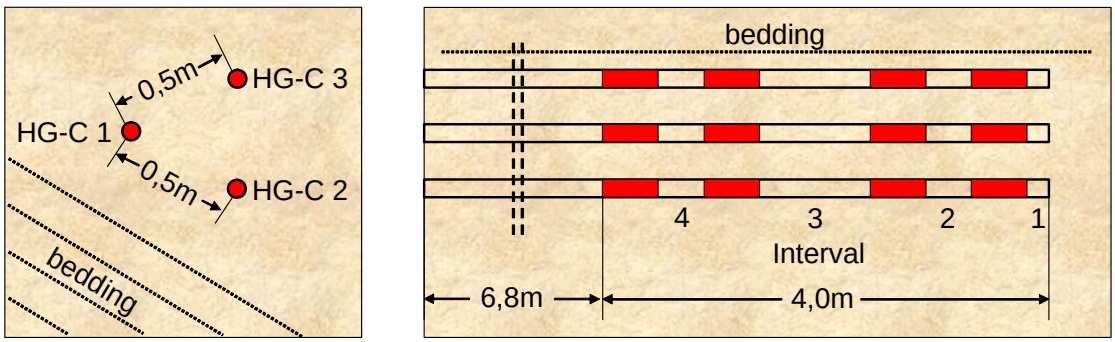

Fig. 4.1 Orientation of the boreholes BHG-C1, BHG-C2, and BHG-C3 parallel to the bedding

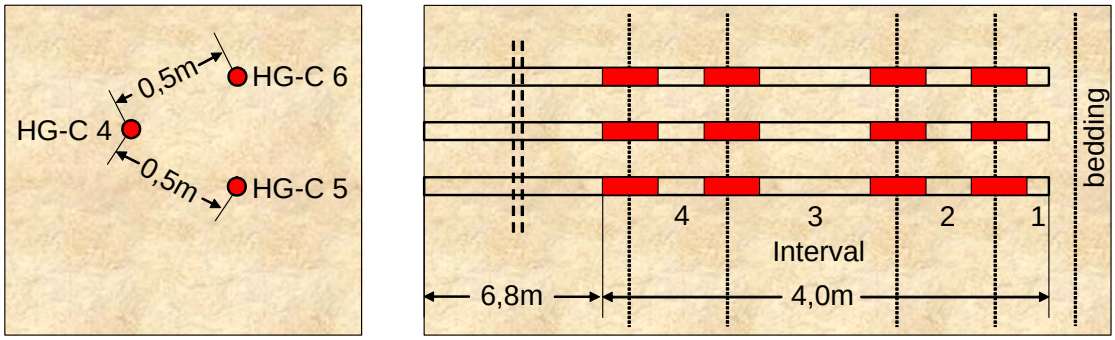

Fig. 4.2 Orientation of the boreholes BHG-C4, BHG-C5, and BHG-C6 perpendicular to the bedding

When the inflation pressure of the packers remained constant at 4.0 MPa and after the Pearson water in all the intervals except those at the deep end of the boreholes (Intervals 1) had been displaced by nitrogen, the intervals BHG-C1/3 (central interval of borehole BHG-C1) and BHG-C4/3 (central interval of borehole BHG-C4) were purged and filled at atmospheric pressure with the gas mixture of 2 vol% of hydrogen, helium, neon, krypton, iso-butane, and sulphur hexafluoride each (tracer gases) within the matrix of 88 vol% nitrogen. After 71 hours the gas in these intervals and in all the other intervals was extracted and the composition with regard to the tracer components was determined by a gas chromatograph. Right after the first extraction the intervals BHG-C1/3 and BHG-C4/3 were purged and filled with the gas mixture again. After 772 to 774 hours (one month) the gas extractions from all the intervals and the analyses were repeated (see Section 5.1).

In a next step, the intervals BHG-C1/3 and BHG-C4/3 were pressurized stepwise to 0.4; 1.1, 1.5; 2.0, 2.5, and 3.0 MPa by injecting the tracer gas mixture. After reaching the envisaged pressure step the intervals were sealed gastight and the pressures in the intervals were recorded for 28 to 50 days. During that time period the pressure decreased as a result of gas solution in the pore water and diffusion in the water of the Opalinus clay or as a result of water displacement and two phase flow in the pore volume. Before inflation to the next step gas samples were taken out of all the intervals for analysis.

For the extraction of a representative gas sample out of the intervals a flow board as shown in Fig. 4.3 was connected to the two capillaries at the valve panel which run to the interval. This flow board consisted of a vacuum pump, a nitrogen bottle, a peristaltic

pump, and a gas sampling bag. First, the internal volume of the flow board was evacuated and purged with nitrogen. Then the system was inflated with nitrogen to 0.15 MPa. If there was no overpressure in the interval it was also inflated to 0.15 MPa by opening the valves to the interval. If there was overpressure in the intervals no further inflation was performed. After opening the valves to the interval and closing the valves of the bypass and to the nitrogen bottle the peristaltic pump purged the system for 30 minutes in a closed circuit to receive a homogenised sample which represents the gas composition in the interval. Then the valves to the sampling bag were opened and the overpressure in the whole system flew into the gas sampling bag. The valves to the interval and of the gas sampling bag were closed. The gas sampling bag was disconnected and sent for analyses by gas chromatograph with regard to the tracer gas components and oxygen to the GRS laboratory in Braunschweig. Oxygen was determined for testing the tightness of the system. The dilution by the injected nitrogen overpressure and by the residual volume of the flow board was taken into account for the determination of the gas concentration in the respective interval (see Section 5.2).

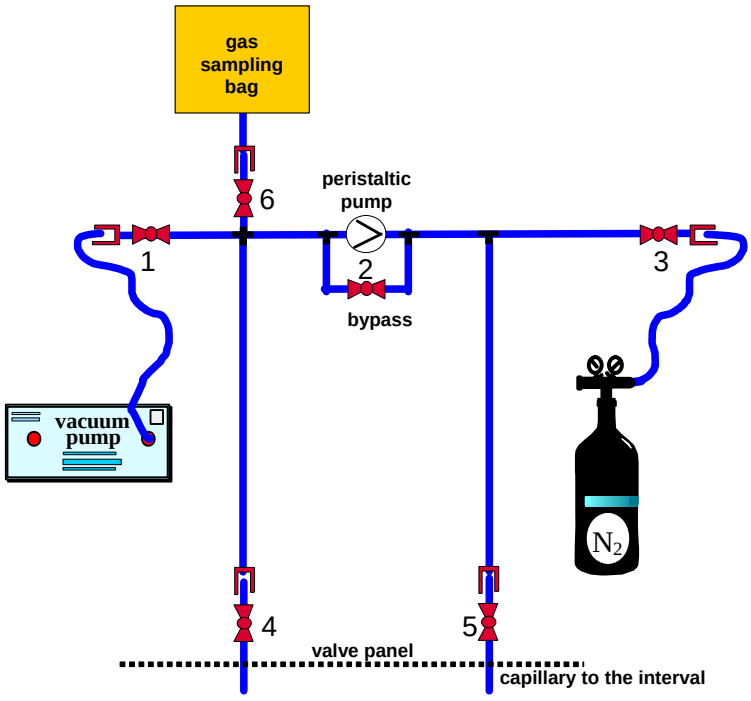

Fig. 4.3 Flow board for gas sampling out of the intervals

Besides the gas samples taken from the injection intervals additionally samples were taken from all the other intervals which were originally purged with nitrogen. By these additional sampling the gas flow from the injection interval into the other intervals was determined.

The concentration decrease of the tracer gases was compared to concentration curves with different diffusion coefficients calculated using the radial-symmetric finite difference code EDIFF in order to estimate the respective diffusion coefficients for the different gases (see Section 5.1 and 5.2). For evaluating the pressure decay curves in terms of permeability, the code WELTEST 200 was used.

WELTEST 200 provides means to calculate the analytic solution to the diffusion equation or to numerically model pressure distribution in one- or two-dimensional models, and to iteratively minimize the deviation between the measured and calculated pressure data. For measurements with gas, the real pressure has to be transformed into the so-called pseudo-pressure m(p) due to the highly pressure-dependent material properties of gas:

$$m(p) = 2\int_{p_i}^{p} \frac{p}{\mu(p)z(p)}\,dp$$

with the initial pressure p_i, the viscosity $\mu(p)$, and the z-factor $z(p)$.

The parameters affecting the calculated pressure evolution are the rock permeability, the rock porosity, the wellbore storage coefficient, and the skin factor. The skin factor accounts for an increased or decreased permeability of a zone close to the borehole wall, which can be due to the drilling procedure. For the HG-C tests, no skin factor was regarded.

The calculated pressure curves are rather insensitive to changes in porosity. The porosity was held constant at 15 %; changing the porosity by a factor of ten has no significant influence on the best fit permeability. Wellbore storage is important during the injection phase and controls the peak pressure reached during injection. The pressure curve form, especially during the shut-in phase, is controlled by the permeability, which, because of the liquid phase in the pore space, represents only an effective permeability at the present saturation conditions. For the measurements at low injection pressure, the best-fit permeability was determined by two-dimensional isotropic calculation.

In a third step, constant head tests were performed. A two litre nitrogen gas bottle was connected to the injection interval maintaining a constant pressure of 1.6 to 3.2 MPa for

some months. The gas bottle was put on a balance in order to determine the gas flow into the interval at the constant gas pressure. The gas pressure in this interval and all the other intervals of the test location as well as the weight of the bottle were recorded continuously by the DAS. In all tests a gas break-through was achieved at a certain pressure, and the gas bottle was then emptied within a comparatively short time (see Section 5.3). The effective permeability after break-through was determined again with WELTEST 200. For these cases, however, a one-dimensional radial flow was assumed, because, as will be shown in Section 5.3, the flow was mostly restricted parallel to the bedding plane.

5 Results

5.1 Intervals Filled with Tracer Gas Mixture and Sealed at Atmospheric Pressure

Measurements for determination of the diffusion coefficients were performed with the components of 2 vol% hydrogen, helium, neon, krypton, iso-butane, and sulphur hexafluoride each in the matrix of 88 vol% nitrogen. This gas mixture was injected into the intervals BHG-C1/3 (parallel to the bedding) and BHG-C4/3 (perpendicular to the bedding) of both test locations at atmospheric pressure. After a time period of 71 and 772 hours, respectively, the gases were extracted from the intervals for analysis and filled again. The quantitative analyses with regard to the tracer gas concentrations were performed at the GRS laboratory in Braunschweig by a gas chromatograph. The differences of the injected and extracted amounts of the tracer gas components are the quotas which have diffused into the surrounding host rock. The results are shown in Tab. 5.1.

Tab. 5.1 Results of the tracer gas injections and extractions with atmospheric pressure into the intervals BHG-C1/3 and BHG-C4/3

Interval BHG-C1/3 - duration between injection and extraction 71 hours

Tracer gas	Injected concentration [vpm]	Injected amount [g]	Extracted concentration [vpm]	Amount in the interval [g]	Quota of diffusion [g]
Hydrogen	20000	1.37E-03	7828	5.36E-04	8.34E-04
Helium	20000	2.72E-03	6035	8.21E-04	1.90E-03
Neon	20000	1.37E-02	14811	1.01E-02	3.55E-03
Iso-butane	20000	4.40E-02	9640	2.12E-02	2.28E-02
Krypton	20000	4.97E-02	15717	3.90E-02	1.06E-02
Sulphur hexafluoride	20000	1.01E-01	16686	8.40E-02	1.67E-02

(Continuation of Tab. 5.1)

Interval BHG-C1/3 - duration between injection and extraction 772 hours

Tracer gas	Injected concentration [vpm]	Injected amount [g]	Extracted concentration [vpm]	Amount in the interval [g]	Quota of diffusion [g]
Hydrogen	20000	1.37E-03	0	0.00E-04	1.37E-03
Helium	20000	2.72E-03	1277	1.74E-04	2.55E-03
Neon	20000	1.37E-02	11680	7.99E-03	5.69E-03
Iso-butane	20000	4.40E-02	5376	1.18E-02	3.22E-02
Krypton	20000	4.97E-02	13163	3.27E-02	1.70E-02
Sulphur hexafluoride	20000	1.01E-01	15285	7.69E-02	2.37E-02

Interval BHG-C4/3 - duration between injection and extraction 71 hours

Tracer gas	Injected concentration [vpm]	Injected amount [g]	Extracted concentration [vpm]	Amount in the interval [g]	Quota of diffusion [g]
Hydrogen	20000	8.34E-04	5768	2.41E-04	5.94E-04
Helium	20000	1.66E-03	5768	4.78E-04	1.18E-03
Neon	20000	8.34E-03	14996	6.25E-03	2.09E-03
Iso-butane	20000	2.68E-02	9311	1.25E-02	1.43E-02
Krypton	20000	3.03E-02	16171	2.45E-02	5.79E-03
Sulphur hexafluoride	20000	6.13E-02	17242	5.29E-02	8.46E-03

Interval BHG-C4/3 - duration between injection and extraction 772 hours

Tracer gas	Injected concentration [vpm]	Injected amount [g]	Extracted concentration [vpm]	Amount in the interval [g]	Quota of diffusion [g]
Hydrogen	20000	8.34E-04	0	0.00E-00	8.34E-04
Helium	20000	1.66E-03	2018	1.67E-04	1.49E-03
Neon	20000	8.34E-03	10279	4.28E-03	4.05E-03
Iso-butane	20000	2.68E-02	9125	1.22E-02	1.46E-02
Krypton	20000	3.03E-02	11659	1.76E-02	1.26E-02
Sulphur hexafluoride	20000	6.13E-02	13225	4.05E-02	2.08E-02

In order to estimate the diffusion coefficient from the measurement results, a one-dimensional radial symmetric finite difference model was used for calculating the concentration curves of a tracer gas component in the test interval for diffusion coefficients of the rock of 10^{-9} m^2/s, 10^{-10} m^2/s, 10^{-11} m^2/s, and 10^{-12} m^2/s over a time

period of 1000 hours. As starting concentration in the boreholes a value of 2.0 vol% (20000 vpm) was chosen for the calculation. This corresponds to the starting concentration of the tracer gas components injected into the residual volume of the boreholes. The Figs. 5.1 and 5.2 show the results of these calculations together with the concentrations measured at BHG-C1/3 and BHG-C4/3, respectively.

The figures show a rather clear dependence of the diffusion velocity on molecular mass, although iso-butane seems to diffuse more quickly than expected. The heavier and “slower” molecules (all except hydrogen and helium) also appear to show lower diffusion coefficients at longer diffusion time. This is, however, an artefact, as will be discussed in Section 5.2.

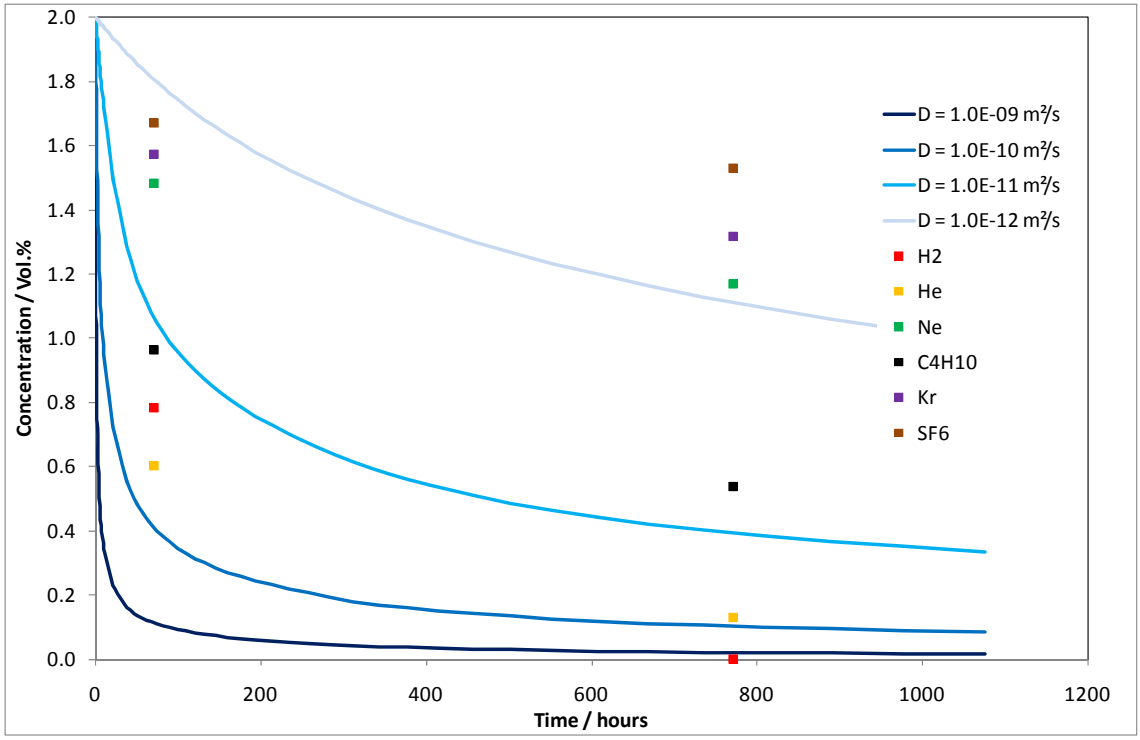

Fig. 5.1 Calculated concentration curves for diffusion coefficients of the rock of 10^{-9} m^2/s, 10^{-10} m^2/s, 10^{-11} m^2/s, and 10^{-12} m^2/s, together with measured concentrations at BHG-C1/3

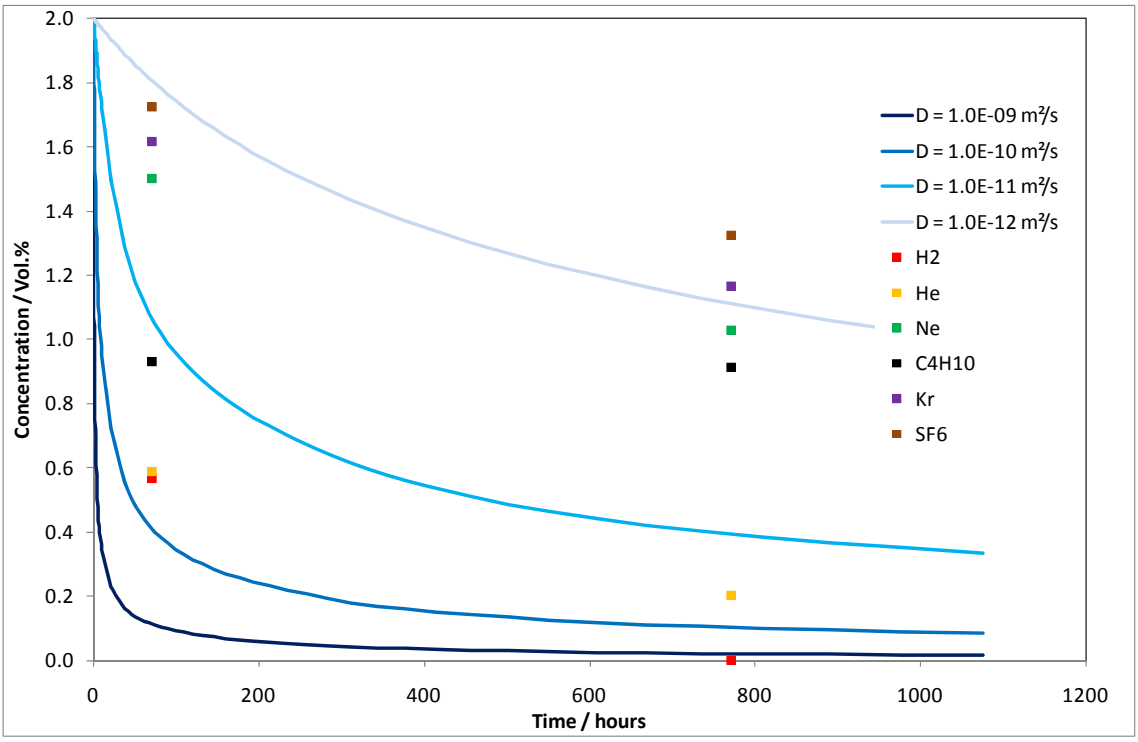

Fig. 5.2 Calculated concentration curves for diffusion coefficients of the rock of 10^{-9} m^2/s, 10^{-10} m^2/s, 10^{-11} m^2/s, and 10^{-12} m^2/s, together with measured concentrations at BHG-C4/3

From the measurements after 71 hours and the calculated concentration curves, the diffusion coefficients for the different tracer gases were identified (see Tab. 5.2). Tab. 5.2 also shows the product $D \cdot \sqrt{M}$, because of the theoretical proportionality between D and $1/\sqrt{M}$ (see Section 4).

The table shows that the reproducibility of the measurement is quite good – there is no systematic difference between the two boreholes. The diffusion coefficients are rather low: By a factor 100 to 1000 lower than the respective diffusivity in water (compare Tab. 4.1). Keeping in mind that the porosity of the rock is only about 15 % and that solubility of the gas and tortuosity of the pore space will have an influence as well, the concentration decrease in the boreholes can be well explained by diffusion in the liquid phase. The results show especially that there is no diffusion in the gas phase, which would imply much higher diffusion coefficients.

Although a dependence of diffusivity on the molecular mass seems obvious, Tab. 5.2 shows that the product $D \cdot \sqrt{M}$ varies between 10^{-10} and 10^{-11} for the different gases.

So, molecular mass alone is not sufficient to describe differences in diffusivity. Other effects, such as sorption of the gases to the internal surfaces and solubility in the interstitial water, seem to influence gas diffusion in the clay rock.

Tab. 5.2 Diffusion coefficients and products $D \cdot \sqrt{M}$ for the different tracer gases

	H_2	**He**	**Ne**	**C_4H_{10}**	**Kr**	**SF_6**
D in m²/s BHG-C1/3	2.5E-11	5E-11	2.6E-12	1.4E-11	2E-12	1.5E-12
D in m²/s BHG-C4/3	5E-11	5E-11	2.5E-12	1.5E-11	1.7E-12	1.2E-12
$D \cdot \sqrt{M}$ BHG-C1/3	3.6E-11	1.0E-10	1.2E-11	1.1E-10	1.8E-11	1.9E-11
$D \cdot \sqrt{M}$ BHG-C4/3	7.1E-11	1.0E-10	1.1E-11	1.2E-10	1.5E-11	1.6E-11

5.2 Intervals Pressurised with Tracer Gas Mixture and Sealed

After the measurement at atmospheric pressure, the intervals BHG-C1/3 and BHG-C4/3 were pressurized stepwise.

BHG-C1/3 was pressurized to 0.24, 0.65, 1.11, 1.52, and 2.02 MPa by injecting the tracer gas mixture. At each envisaged pressure step the intervals were sealed gastight and the pressure in the interval was recorded for 28 to 50 days. During these time periods the pressure decreased as a result of gas solution in the pore water and diffusion in the water of the Opalinus clay or as a result of water displacement and two phase flow in the pore volume. Before inflation to the next step gas samples were taken from all the intervals for analysis. Tab. 5.3 shows the pressure and concentration data for each pressure step. Fig. 5-3 shows the gas pressure decay in the injection interval BHG-C1/3 for each step.

Tab. 5.3 Data of gas migration in the interval BHG-C 1/3 (parallel to bedding). Volume of the test interval: 814 cm^3, surface of the test volume to the host rock: 1193 cm^2

Pressure of inflation: 0.24 MPa
Pressure before extraction: 0.23 MPa
Duration between inflation and extraction 617 hours

Tracer gas	Injected concentration [vpm]	Amount in the interval after injection [g]	Amount in the interval before extraction [g]	Quota of migration [g]
Hydrogen	20000	3.29E-03	2.28E-05	3.26E-03
Helium	20000	6.53E-03	3.70E-03	2.82E-03
Neon	20000	3.28E-02	2.82E-02	4.67E-03
Iso-butane	20000	1.06E-01	6.06E-02	4.49E-02
Krypton	20000	1.19E-01	9.67E-02	2.26E-02
Sulphur hexafl.	20000	2.42E-01	2.24E-01	1.74E-02

Pressure of inflation: 0.65 MPa
Pressure before extraction: 0.60 MPa
Duration between inflation and extraction 672 hours

Tracer gas	Injected concentration [vpm]	Amount in the interval after injection [g]	Amount in the interval before extraction [g]	Quota of migration [g]
Hydrogen	20000	8.90E-03	0.00E-00	8.90E-03
Helium	20000	1.77E-02	1.25E-02	5.20E-03
Neon	20000	8.89E-02	7.86E-02	1.03E-02
Iso-butane	20000	2.86E-01	1.62E-01	1.24E-01
Krypton	20000	3.23E-01	2.57E-01	6.63E-02
Sulphur hexafl.	20000	6.54E-01	6.02E-01	5.24E-02

Pressure of inflation: 1.11 MPa
Pressure before extraction: 0.96 MPa
Duration between inflation and extraction 1176 hours

Tracer gas	Injected concentration [vpm]	Amount in the interval after injection [g]	Amount in the interval before extraction [g]	Quota of migration [g]
Hydrogen	20000	1.52E-02	0.00E-00	1.52E-02
Helium	20000	3.02E-02	1.59E-02	1.42E-02
Neon	20000	1.52E-01	1.21E-01	3.04E-02
Iso-butane	20000	4.88E-01	2.62E-01	2.26E-01
Krypton	20000	5.51E-01	4.03E-01	1.48E-01
Sulphur hexafl.	20000	1.12E-00	9.78E-01	1.39E-01

(Continuation of Tab. 5.3)

Pressure of inflation: 1.52 MPa
Pressure before extraction: 1.39 MPa
Duration between inflation and extraction 816 hours

Tracer gas	Injected concentration [vpm]	Amount in the interval after injection [g]	Amount in the interval before extraction [g]	Quota of migration [g]
Hydrogen	20000	2.08E-02	1.11E-02	9.68E-03
Helium	20000	4.13E-02	2.42E-02	1.71E-02
Neon	20000	2.08E-01	1.74E-01	3.37E-02
Iso-butane	20000	6.68E-01	4.23E-01	2.45E-01
Krypton	20000	7.55E-01	6.03E-01	1.52E-01
Sulphur hexafl.	20000	1.53E-00	1.39E-00	1.40E-01

Pressure of inflation: 2.02 MPa
Pressure before extraction: 1.78 MPa
Duration between inflation and extraction 980 hours

Tracer gas	Injected concentration [vpm]	Amount in the interval after injection [g]	Amount in the interval before extraction [g]	Quota of migration [g]
Hydrogen	20000	2.77E-02	1.67E-02	1.10E-02
Helium	20000	5.50E-02	3.52E-02	1.98E-02
Neon	20000	2.77E-01	2.29E-01	4.78E-02
Iso-butane	20000	8.89E-01	5.78E-01	3.11E-01
Krypton	20000	1.00E-00	7.78E-01	2.27E-01
Sulphur hexafl.	20000	2.04E-00	1.80E-00	2.35E-01

BHG-C4/3 was pressurized to 0.23 and 0.59 MPa. When a break-through to the interval BHG-C5/3 was detected at this low pressure, it was decided to use the uninfluenced BGH-C6-3 for the further pressure steps of 1.14, 1.56, 2.01, 2.51, and 3.02 MPa. The reason for the breakthrough between BHG-C4/3 and BHG-C5/3 at this low pressure is probably a weak zone along the bedding between the two boreholes. It has to be quite restricted in extent, since BGH-C6-3 was not influenced.

Fig. 5.4 shows the gas pressure decay in the injection intervals BHG-C4/3 and BHG-C6/3 for each step, respectively. Tab. 5.4 shows the pressure and concentration data for each pressure step.

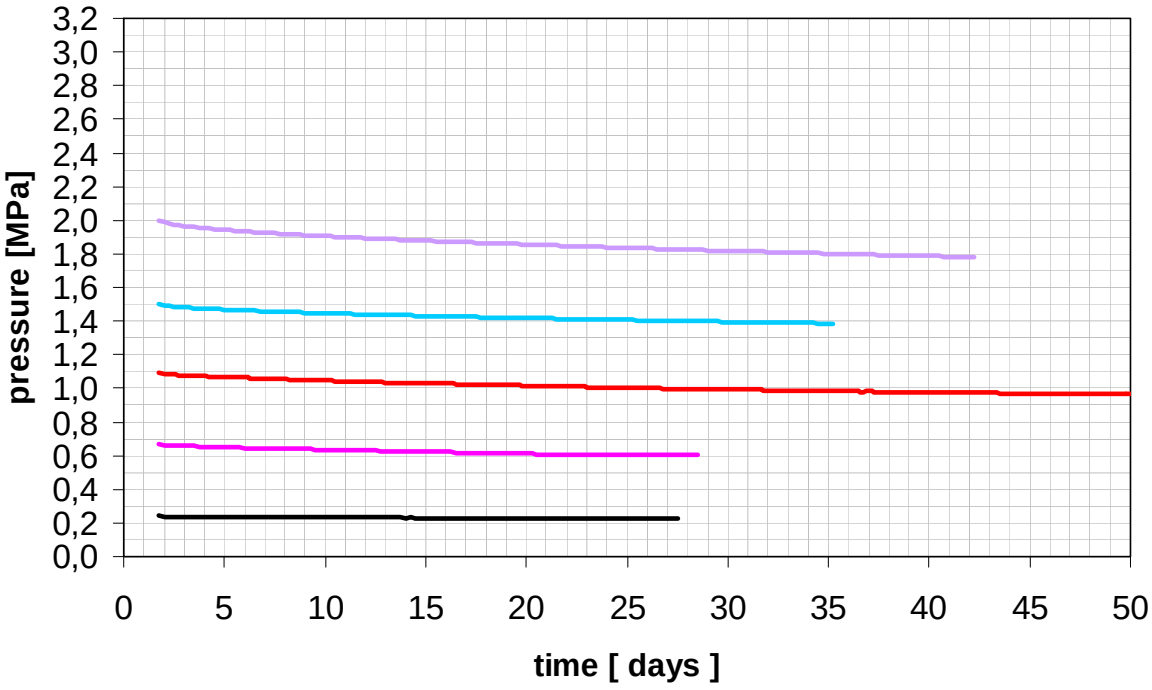

Fig. 5.3 Pressure trends in the intervals BHG-C1/3 (borehole parallel to the bedding), pressure steps between 0.24 and 2.02 MPa

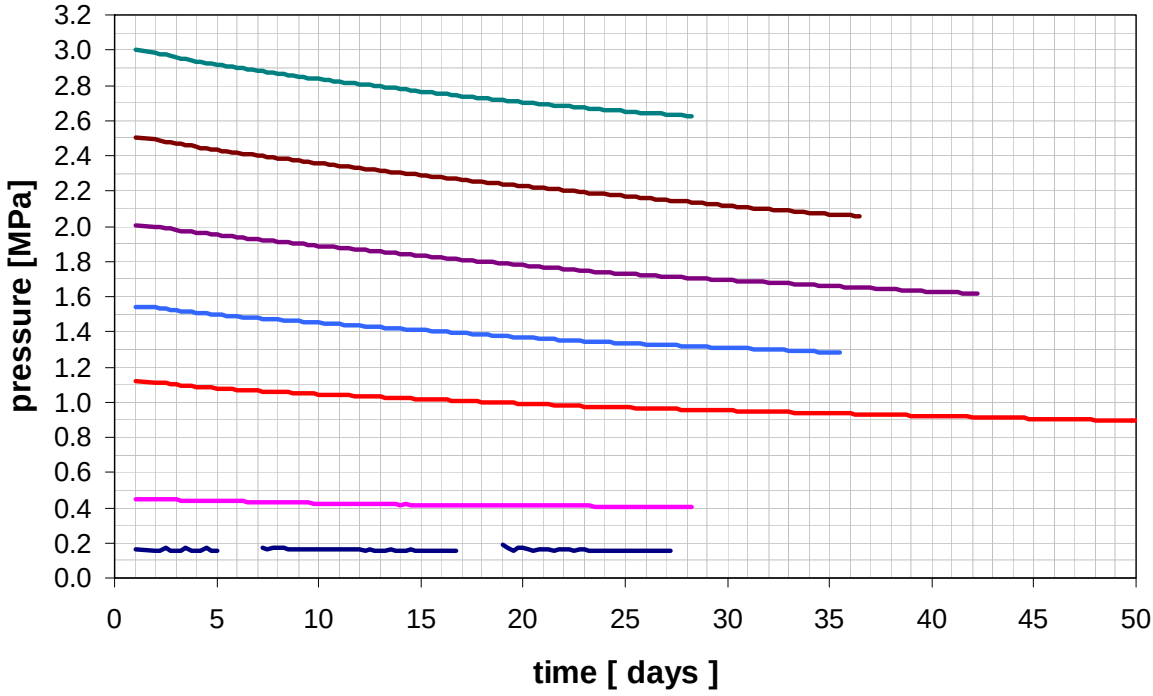

Fig. 5.4 Pressure trends in the intervals BHG-C4/3 and BHG-C6/3 (boreholes perpendicular to the bedding), pressure steps between 0.18 and 3.0 MPa

Tab. 5.4 Data of gas migration in the intervals BHG-C4/3 and BHG-C 6/3 (perpendicular to bedding). Volume of the test interval: 892 cm^3, surface of the test volume to the host rock: 1193 cm^2

Pressure of inflation: 0.23 MPa
Pressure before extraction: 0.16 MPa
Duration between inflation and extraction 617 hours

Tracer gas	Injected concentration [vpm]	Amount in the interval after injection [g]	Amount in the interval before extraction [g]	Quota of migration [g]
Hydrogen	20000	1.92E-03	0.00E-00	1.92E-03
Helium	20000	3.81E-03	7.20E-04	3.09E-03
Neon	20000	1.92E-02	1.08E-02	8.39E-02
Iso-butane	20000	6.16E-02	2.99E-02	3.17E-02
Krypton	20000	6.96E-02	4.02E-02	2.94E-02
Sulphur hexafl.	20000	1.41E-01	9.16E-02	4.94E-02

Pressure of inflation: 0.59 MPa
Pressure before extraction: 0.41 MPa
Duration between inflation and extraction 672 hours

Tracer gas	Injected concentration [vpm]	Amount in the interval after injection [g]	Amount in the interval before extraction [g]	Quota of migration [g]
Hydrogen	20000	4.92E-03	1.86E-06	4.92E-03
Helium	20000	9.78E-03	4.61E-03	5.17E-03
Neon	20000	4.92E-02	3.12E-02	1.80E-02
Iso-butane	20000	1.58E-01	8.27E-02	7.54E-02
Krypton	20000	1.79E-01	1.04E-01	7.47E-02
Sulphur hexafl.	20000	3.62E-01	2.48E-01	1.14E-01

Pressure of inflation: 1.14 MPa
Pressure before extraction: 0.89 MPa
Duration between inflation and extraction 1176 hours

Tracer gas	Injected concentration [vpm]	Amount in the interval after injection [g]	Amount in the interval before extraction [g]	Quota of migration [g]
Hydrogen	20000	1.71E-02	0.00E-00	1.71E-02
Helium	20000	3.39E-02	1.53E-02	1.86E-02
Neon	20000	1.70E-01	1.22E-01	4.89E-02
Iso-butane	20000	5.48E-01	2.92E-01	2.56E-01
Krypton	20000	6.19E-01	3.89E-01	2.30E-01
Sulphur hexafl.	20000	1.25E-00	9.93E-01	2.62E-01

(Continuation of Tab. 5.4)

Pressure of inflation: 1.56 MPa
Pressure before extraction: 1.28 MPa
Duration between inflation and extraction 816 hours

Tracer gas	Injected concentration [vpm]	Amount in the interval after injection [g]	Amount in the interval before extraction [g]	Quota of migration [g]
Hydrogen	20000	2.34E-02	0.00E-00	2.34E-02
Helium	20000	4.65E-02	2.21E-02	2.44E-02
Neon	20000	2.34E-01	1.74E-01	5.99E-02
Iso-butane	20000	7.52E-01	5.04E-01	2.48E-01
Krypton	20000	8.50E-01	6.15E-01	2.34E-01
Sulphur hexafl.	20000	1.72E-00	1.44E-00	2.87E-01

Pressure of inflation: 2.01 MPa
Pressure before extraction: 1.61 MPa
Duration between inflation and extraction 980 hours

Tracer gas	Injected concentration [vpm]	Amount in the interval after injection [g]	Amount in the interval before extraction [g]	Quota of migration [g]
Hydrogen	20000	3.02E-02	0.00E-00	3.02E-02
Helium	20000	6.00E-02	3.53E-02	2.47E-02
Neon	20000	3.02E-01	2.25E-01	7.66E-02
Iso-butane	20000	9.66E-01	6.64E-01	3.03E-01
Krypton	20000	1.10E-00	7.96E-01	3.00E-01
Sulphur hexafl.	20000	2.22E-00	1.78E-00	4.42E-01

Pressure of inflation: 2.51 MPa
Pressure before extraction: 2.06 MPa
Duration between inflation and extraction 838 hours

Tracer gas	Injected concentration [vpm]	Amount in the interval after injection [g]	Amount in the interval before extraction [g]	Quota of migration [g]
Hydrogen	20000	3.77E-02	0.00E-00	3.77E-02
Helium	20000	7.48E-02	5.03E-02	2.45E-02
Neon	20000	3.76E-01	2.79E-01	9.71E-02
Iso-butane	20000	1.21E-00	8.78E-01	3.37E-01
Krypton	20000	1.37E-00	1.01E-00	3.58E-01
Sulphur hexafl.	20000	2.77E-00	2.20E-00	5.67E-01

(Continuation of Tab. 5.4)

Pressure of inflation: 3.02 MPa
Pressure before extraction: 2.57 MPa
Duration between inflation and extraction 840 hours

Tracer gas	Injected concentration [vpm]	Amount in the interval after injection [g]	Amount in the interval before extraction [g]	Quota of migration [g]
Hydrogen	20000	4.54E-02	2.03E-02	2.50E-02
Helium	20000	9.01E-02	5.70E-02	3.31E-02
Neon	20000	4.53E-01	3.67E-01	8.61E-02
Iso-butane	20000	1.45E-00	1.02E-00	4.27E-01
Krypton	20000	1.65E-00	1.32E-00	3.23E-01
Sulphur hexafl.	20000	3.33E-00	2.87E-00	4.63E-01

The pressure decay may be the result of the two complementary gas migration effects in the clay:

1. Solution of the tracer gas components in the interstitial water of the clay and diffusion of these components in the water of the surrounding host rock, as it was found at ambient pressure.

2. Advection in a non water saturated pore volume of the clay.

For evaluating the measurements under the assumption of diffusion in the liquid phase, the mass data of the different tracer gases were transformed into equivalent concentration data for ambient pressure. Then, these concentrations with their respective diffusion times were compared to the calculated concentration curves for different diffusivities presented in Section 5.1. Fig. 5.5 shows the results for the helium concentrations.

It can be seen that the measured diffusivity values seem to cover a large range between 10^{-10} and $<10^{-12}$ m²/s. The tracer injections, however, were performed one after the other, and therefore, prior to each measurement, the pore space was already contaminated by all the preceding injections. Consequently, the concentration gradient is lower and the diffusion is slowed down. This is not accounted for in the calculation. As a consequence, there is a general trend in the values to lower apparent diffusivities, which is visualised in Fig. 5.5 by the arrows showing the succession of measurements.

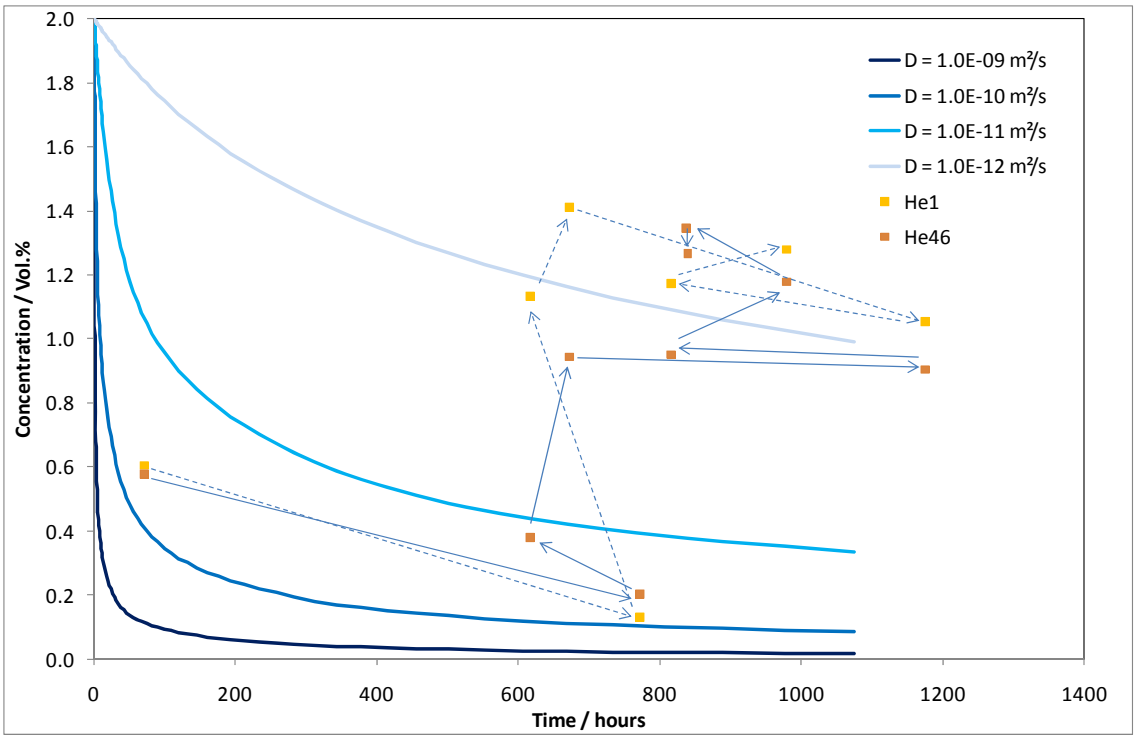

Fig. 5.5 Calculated concentration curves for diffusion coefficients of the rock of 10^{-9} m^2/s, 10^{-10} m^2/s, 10^{-11} m^2/s, and 10^{-12} m^2/s, together with measured concentrations of helium at BHG-C1/3 (He1) and BHG-C4/3 and 6/3 (He46). The arrows show the succession of measurements

For the above reason, only the first measurements yield correct values of the diffusivity. The trend to lower apparent diffusivities because of existing concentrations in the rock is consistent with the assumption that diffusion is the main migration mechanism at low pressures. It is visible with the other tracer gases as well, for the components with higher molecular mass it could already be seen with the first two successive measurements at ambient pressure (see Section 5.1).

In particular, the low values imply that there is no gas phase which would lead to much higher diffusion coefficients (see Tab. 4.1).

It would be worthwile to model the whole test history with the succession of the various injections to demonstrate that the measured concentrations can be explained by one diffusion coefficient for each tracer component. This could, however, not be performed in the frame of the HG-C.

The discussion above showed that the existence of a gas phase is rather unlikely. As a consequence, it can be expected that evaluating the measured pressure curves in

terms of effective gas permeability will probably lead to very low values. In fact, only the first measurements at the lowest injection pressure were evaluable at all (see Fig. 5.6 for an example). They led to the extreme low permeabilities of 10^{-22} m^2. For the other measurements, effective permeability was so low that the evaluation code became unstable. From the curve forms, however, it can be deduced that there is a trend to lower permeability with higher injection pressure. There is no logic explanation for such behaviour. In fact, this together with the diffusion interpretation shows (not surprisingly) that advection is not a mechanism that has to be considered in the undisturbed water saturated clay rock.

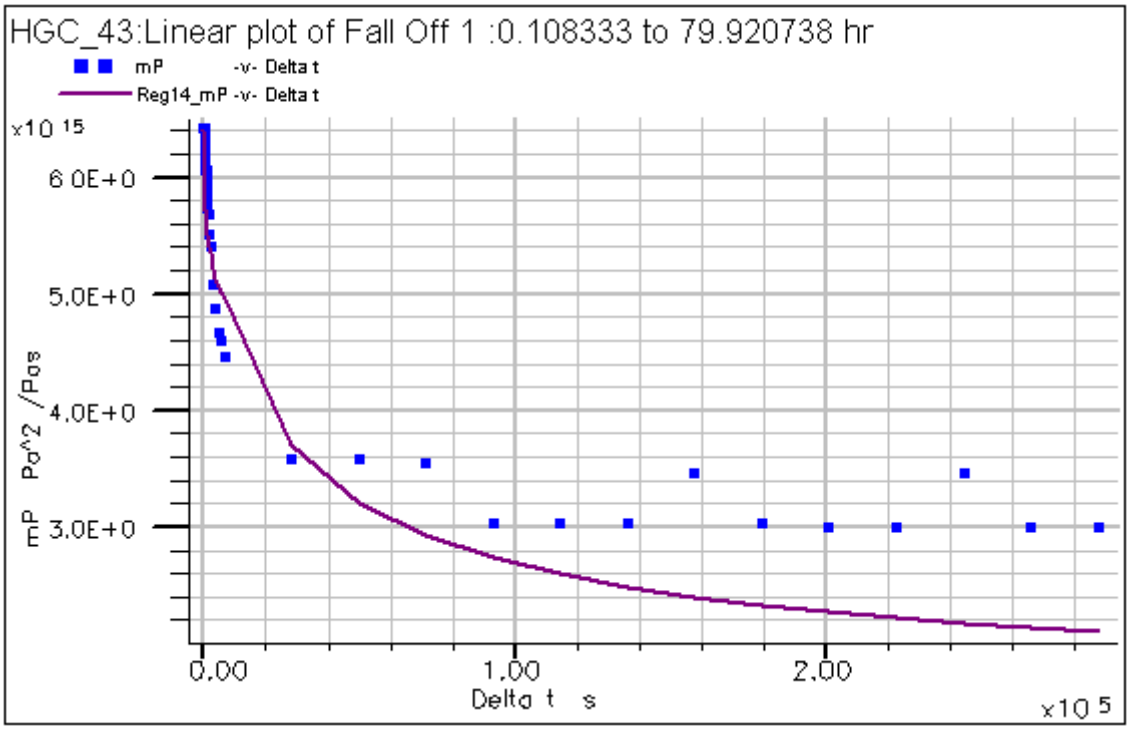

Fig. 5.6 Measurement values of the injection to 0.24 MPa at BHG-C4/3 transformed into pseudo-pressures (blue) and fitted WELTEST 200 evaluation curve (purple) for an effective permeability of 10^{-22} m^2

5.3 Constant Head Tests at Elevated Pressure

In order to determine the gas entry pressure at which a significant advective gas flow sets in the intervals were again pressurized stepwise with constant pressure via a gas bottle with adjustable pressure reducing valve. The gas flow into the interval was determined by weighing the gas bottle continuously. The data were recorded by the DAS.

Five different intervals (BHG-C1/3 and BHG-C3/2 parallel and BHG-C6/2, BHG-C6/3, and BHG-C6/4 perpendicular to the bedding), were used for a total of ten constant pressure injection tests.

Interval BHG-C1/3

The interval was pressurized stepwise up to 2.2 MPa, at which pressure a sudden gas flow into the surrounding host rock was observed. As a result of that gas flow the gas pressures in the intervals BHG-C1/1, BGH-C1/2, BGH-C2/1, BGH-C2/2, and BGH-C3/1 increased (see Fig. 5.7), while the gas pressures in the other intervals of the boreholes BHG-C1, BHG-C2 and BHG-C3 were not influenced. This means that the preferential path of the gas was parallel to the bedding planes (from interval BHG-C 1/3 into the intervals BHG-C1/1, BGH-C1/2, BGH-C 2/1, BGH-C 2/2, see Fig. 4.1 for the orientation of the boreholes with respect to the bedding). Only one influenced interval, BGH-C3/1, lies outside the bedding plane.

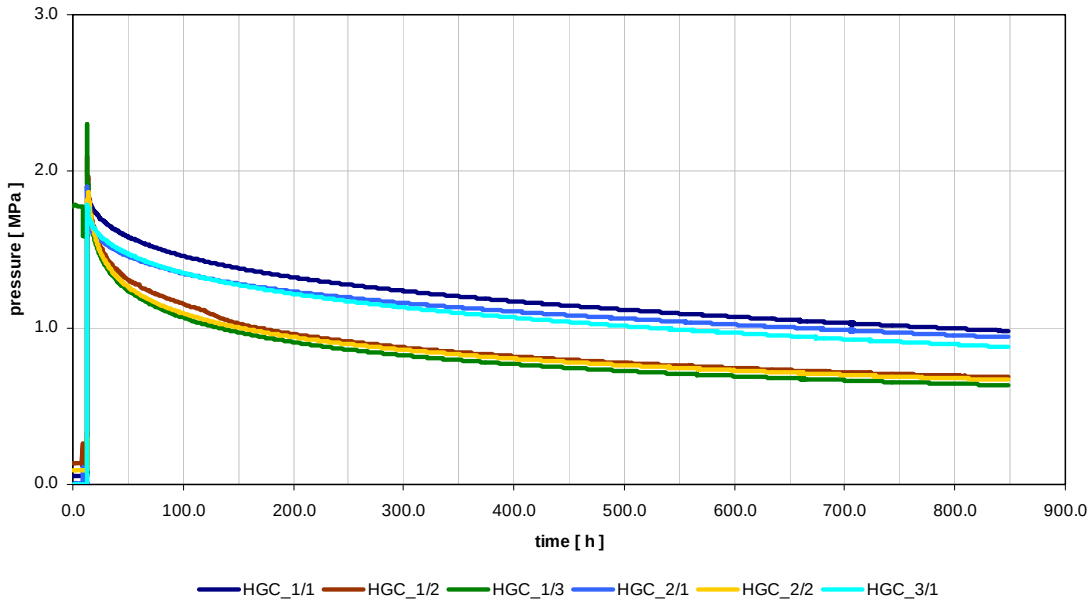

Fig. 5.7 Injection test with nitrogen at BHG-C1/3: Gas break-through at 2.2 MPa to BHG-C1/1, BHG-C1/2, BHG-C2/1, BHG-C2/2, and BHG-C3/1

10 minutes after break-through the gas injection into the interval BHG-C1/3 was stopped and the interval was sealed gastight. The gas pressures in the intervals of the boreholes BHG-C1, BHG-C2 and BHG-C3 were recorded for another 850 hours. During that time period the gas pressure decreased to the range of 1.0 MPa in the

intervals BGH-C1/1, BGH-C2/1, and BGH-C3/1 and to 0.6 MPa in the intervals BGH-C1/2, BGH-C1/3, and BGH-C 2/2, respectively.

A second pressure test at interval BHG-C1/3 (Fig. 5.8) was performed 140 days after the first one. In this case the gas flow was determined by weighing the gas bottle. With a short time delay the gas pressure in interval BHG-C1/2 increased almost to the level of the inflation pressure which indicates that a short-cut along the along the bedding plane had remained from the previous test. Already at 1.1 MPa within 5.2 hours 10.1 g of gas flowed with no significant pressure increase in all the other intervals except BHG-C1/2. At the injection pressure of 1.6 MPa 43.0 g of gas flowed within 17.38 hours, and the pressures in the intervals BHG-C2/1 and BHG-C2/2 increased, indicating the gas flow along the bedding planes. At the injection pressure of 1.8 MPa 20.0 g of gas flowed within 17.38 hours. Again the pressures in the intervals BHG-C2/1, BHG-C2/2, and BHG-C1/2 increased as well.

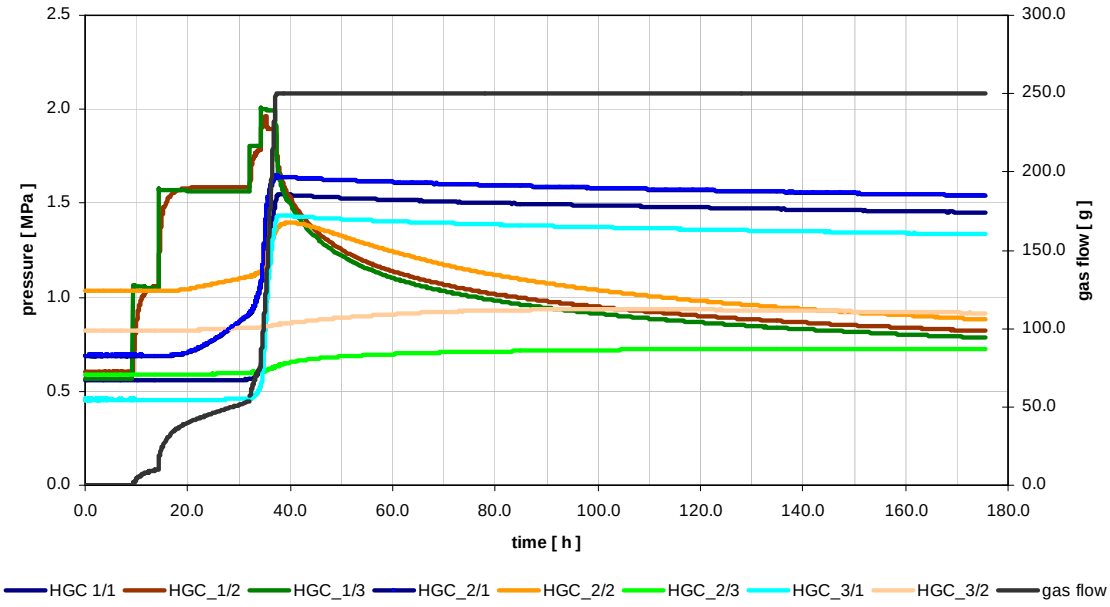

Fig. 5.8 Second injection test at interval BHG-C1/3 (140 days after the first one): Gas break-through at 2.0 MPa to BHG-C1/1, BHG-C1/2, BHG-C2/1, BHG-C2/2, BHG-C2/3, BHG-C3/1, and BHG-C3/2

At the pressure step 2.0 MPa the gas flow increased drastically (175.2 g in 4.17 hours). As a result of that gas break-through the gas pressures increased in the intervals BHG-C1/1, BHG-C1/2, BHG-C2/1, BHG-C2/2, BHG-C2/3, BHG-C3/1, and BHG-C3/2.

This second test showed that the host rock was already disturbed by the first one, which resulted in a lower gas break-through pressure. The original conditions had not been restored within the time period of 140 days between the first and the second test.

From the pressure curves it is not clear whether the mechanism leading to increased flow is the formation of microfractures or the displacement of pore water without mechanical interaction. Macrofracturing, however, can most probably be excluded, because there is always a delay in the pressure reaction of the influenced intervals to the pressure in the injection interval. The flow mechanism at elevated pressure is, however, the main interest of the BET project, and the HG-C data will be used for this project as well.

The code WELTEST was used to estimate the effective permeability of the rock to the gas after break-through (see Fig. 5.9). The evaluation yielded a value of $7 \cdot 10^{-19}$ m^2. It has to be noted that the flow geometry is not covered well by the WELTEST model for the injection borehole parallel to the bedding plane. Consequently, the fit is not extremely good, and the effective permeability value can only be seen as an estimate.

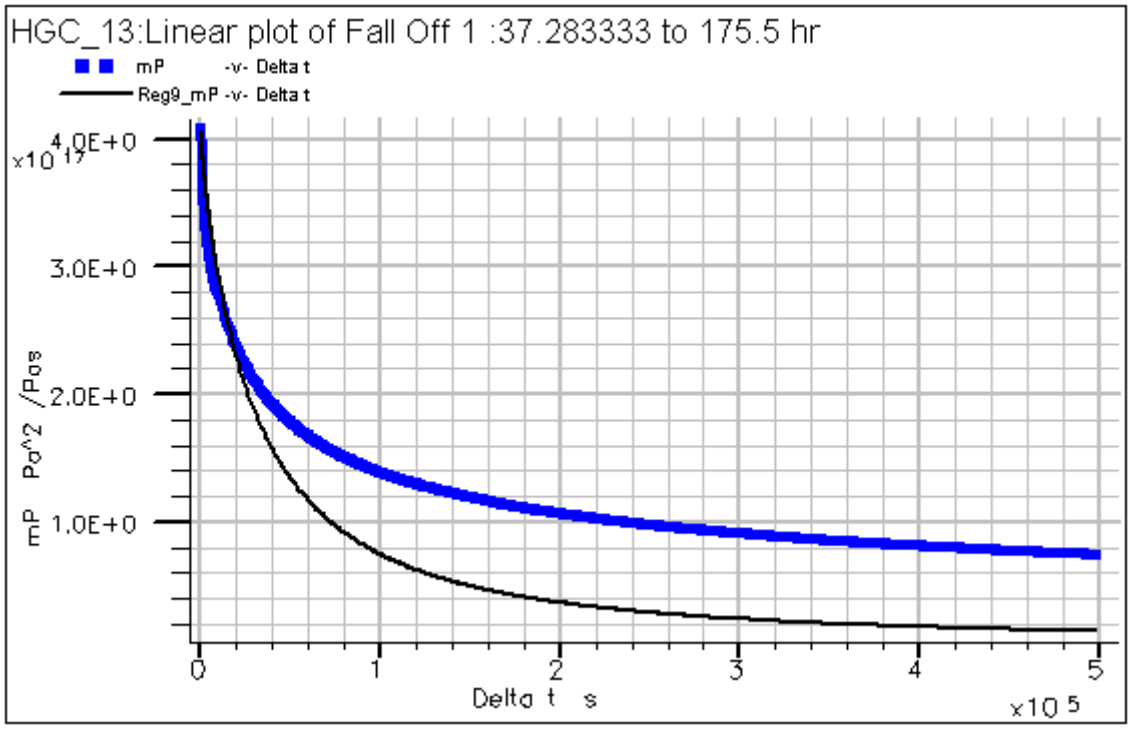

Fig. 5.9 Second injection at BHG-C1/3: Measured pressure decay after break-through transformed into pseudo-pressure (blue) and fitted evaluation curve (black) for an effective permeability of $7 \cdot 10^{-19}$ m^2

Interval BHG-C3/2

The interval was pressurized stepwise, and at a pressure of 1.92 MPa a break-through to BGH-C2/2 was observed – but nearly 2 hours after the pressure step had been reached. This delay is a clear hint against macrofracturing (see above). Then 110.3 g of gas flew into the surrounding host rock in 8.97 hours. Besides BGH-C2/2, the pressure increased at BGH-C1/2, BGH-C1/3, and BGH-C2/3. At time 12 hours in Fig. 5.10 the flow rate reduced because of low gas bottle pressure, and at time 24 hours, the bottle was empty.

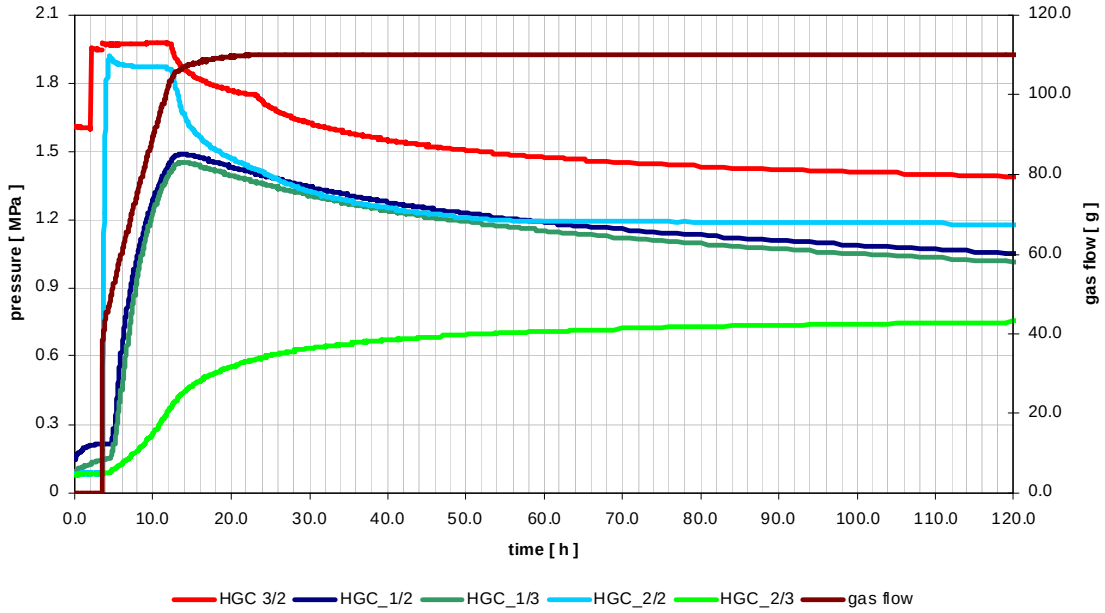

Fig. 5.10 Injection test at interval BHG-C3/2: Gas break-through at 1.92 MPa to BHG-C2/2, BHG-C1/2, BHG-C1/3, and BHG-C2/3

In this case, gas flowed from BHG-C3 to BHG-C2 and BHG-C1 perpendicular to the bedding – probably as a consequence of the injection tests at BHG-C1/3.

A second stepwise injection test at interval BHG-C3/2 was performed 148 days after the first one (Fig. 5.11). A gas break-through to BHG-C2/2 was already observed at 1.75 MPa and within 25 hours 171 g of gas flowed into the surrounding host rock. With a short time delay the gas pressure in interval BHG-C2/2 increased almost to the level of the inflation pressure. After the gas break-through the gas pressure in the intervals BHG-C1/2, BHG-C1/3, and BHG-C2/3 increased to levels between 0.7 and 0.9 MPa.

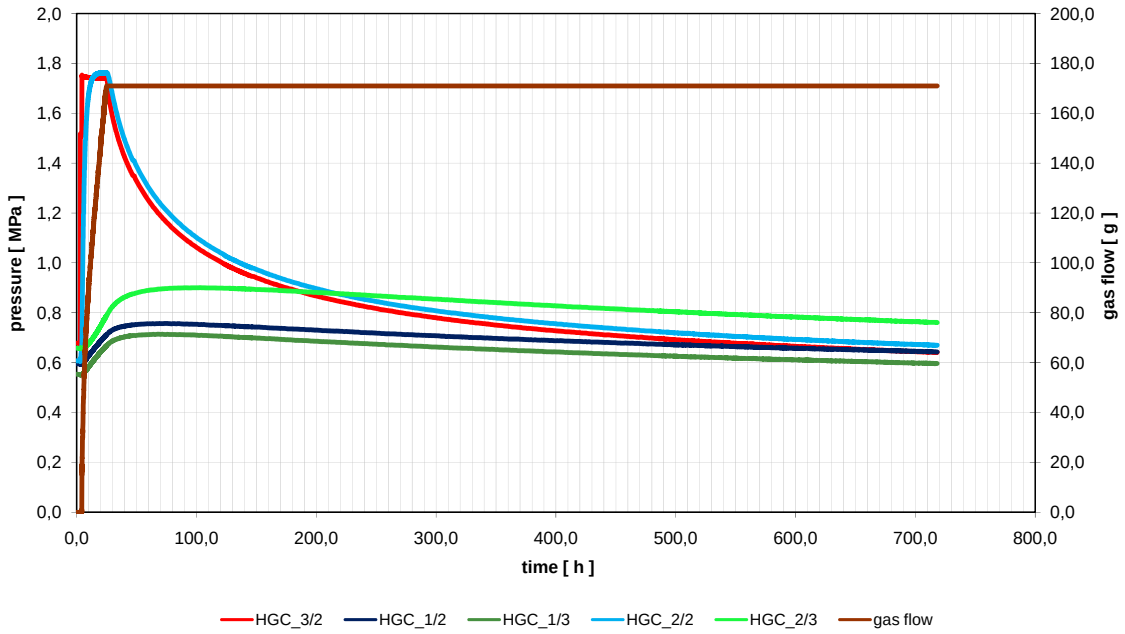

Fig. 5.11 Second injection test at interval BHG-C3/2 (148 days after the first one): Gas break-through at 1.75 MPa to BHG-C2/2

As in the tests performed at BHG-C1/3, the second break-through occurs at a somewhat lower pressure, which shows that the original state was not reached in 148 days.

The two injection tests were evaluated in terms of effective permeability. For the first test, no satisfying agreement could be found, while the second yielded a good fit with an effective permeability value of $3 \cdot 10^{-19}$ m^2.

Interval BHG-C6/2

The interval was pressurized stepwise to 3.2 MPa, then the gas pressure in the interval was held constant. Within 296.5 hours only 3.8 g of gas were lost to the surrounding host. After 296.5 hours a sudden gas break-through to BHG-C5/2 was observed and within 15 hours 72.1 g of gas flowed into the rock and BHG-C5/2 (Fig. 5.12). All other intervals of the boreholes BGH-C4, BGH-C5 and BGH-C6 were not influenced by the gas injection. This means that gas flew parallel to the bedding planes into the rock (see Fig. 4.2 for the orientation of the boreholes perpendicular to the bedding).

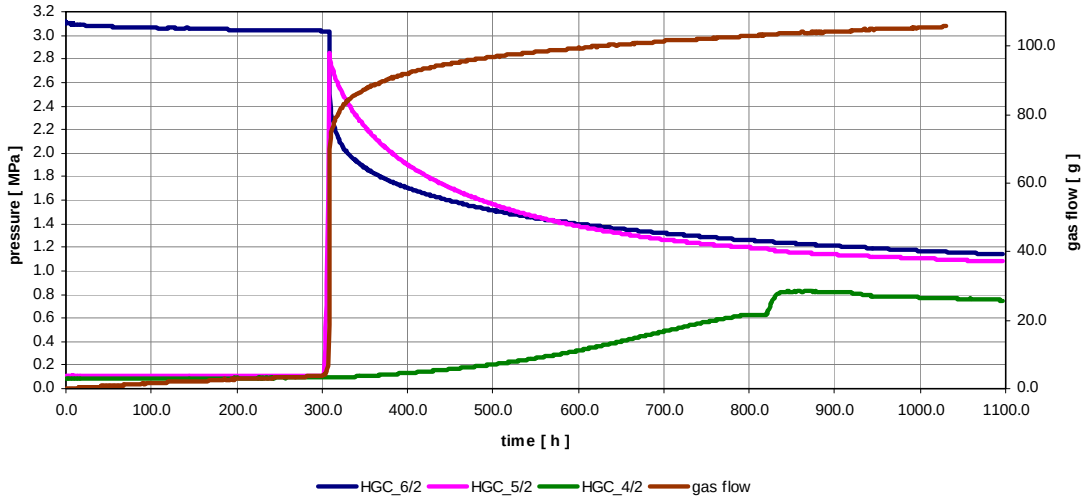

Fig. 5.12 Injection test at interval BHG-C6/2: Gas break-through at 3.2 MPa to BHG-C5/2

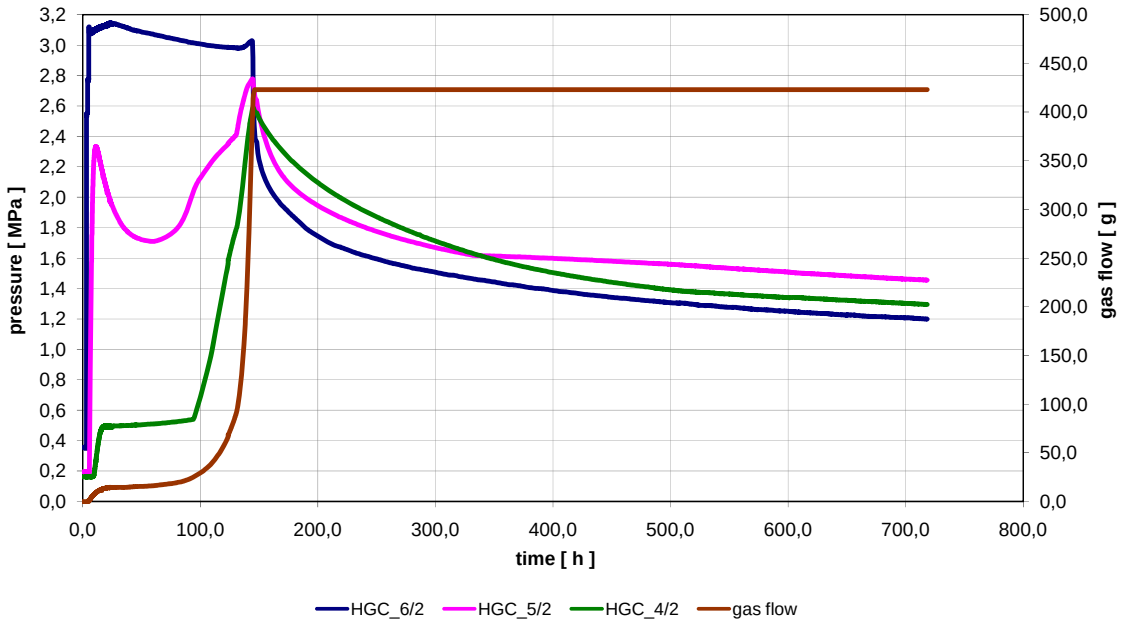

Fig. 5.13 Second injection test at interval BHG-C6/2 (203 days after the first one): Gas break-through at 3.1 MPa to BHG-C5/2 and BHG-C4/2

A second injection test at interval BHG-C6/2 was performed 203 days after the first one. At 3.1 MPa a gas flow along the bedding planes to the intervals BHG-C5/2 and BHG-C4/2 was detected (Fig. 5.13). Flow accelerated only after 100 hours, and the pressure in the intervals BHG-C5/2 andBHG-C4/2 increased to almost 2.8 MPa. When the gas bottle became empty the gas pressure in all three intervals reduced to the range of 1.2 to 1.5 MPa as a result of the gas flow into the surrounding host rock.

As in the tests performed at the other boreholes, the original state was not reached during the time between the two injections. Flow was restricted parallel to the bedding planes.

The effective gas permeability determined for the injection test performed at BHG-C6/2 was 10^{-19} m^2.

Interval BHG-C6/3

The interval was pressurized to 3.0 MPa. For 833 hours no gas flow was observed, but the pressure in the interval decreased within that time period to 2.6 MPa (Fig. 5.14). Then a gas break-through to BHG-C5/3 and BHG-C4/3 occurred and within 11 hours about 166.6 g of gas flowed into the rock until the gas bottle was empty. Afterward gas flowed into the surrounding host rock which led to a pressure decrease in the injection interval BHG-C6/3 to 0.8 MPa and in the intervals BGH-C5/3 and BHG-C4/3 to 1.4 MPa. Note that the pressure in these two intervals is always nearly identical. This is a consequence of the short-cut detected already during the low-pressure injection tests (see Section 5.2).

All the other intervals of the boreholes BGH-C 4, BGH-C 5 and BGH-C 6 were not influenced by this gas injection. Again, gas flow was parallel to the bedding planes.

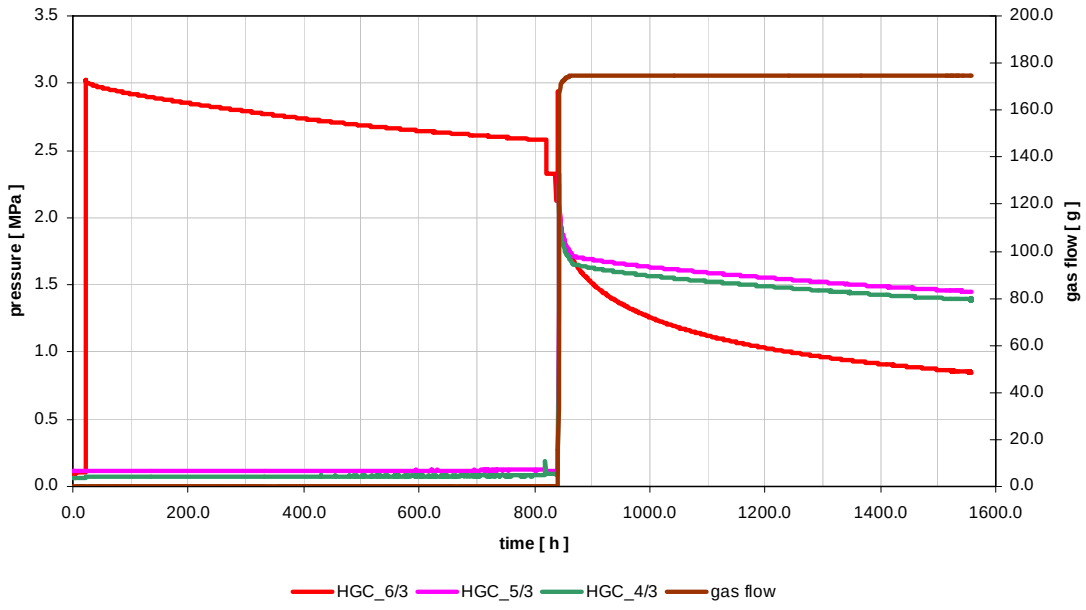

Fig. 5.14 Injection test at interval BHG-C6/3: Gas break-through at 2.6 MPa to BHG-C5/3 and BHG-C4/3

A second stepwise injection test of interval BHG-C6/3 was performed 223 days after the first one (Fig. 5.15). Already at a pressure of 2.0 MPa a gas flow along the bedding layers to the intervals BHG-C5/3 and BHG-C4/3 was detected. The injection pressure was held constant for 5.83 hours. Within that time period 23.5 g of gas flowed into the rock. The pressure in the intervals BHG-C5/3 and BHG-C4/3 increased to almost 0.7 MPa during this time. Then the injection was stopped and the intervals were sealed. The gas pressure in all three intervals equilibrated to about 1.0 MPa. Later, the pressure at BHG-C6/3 decreased further, while it remained constant at BHG-C5/3 and BHG-C4/3. This means that the flow path between the intervals was sealed again at the lower gas pressure, otherwise, all three intervals should have shown the same pressure evolution. The same effect can be seen in Fig. 5.14 at a higher pressure level (1.6 MPa). It seems a hydromechanic interaction with opening and closing pathways as a consequence of the pressure distribution (dilatancy controlled gas flow) is more likely than a pure hydraulic explanation with water displacement by the gas (two-phase flow).

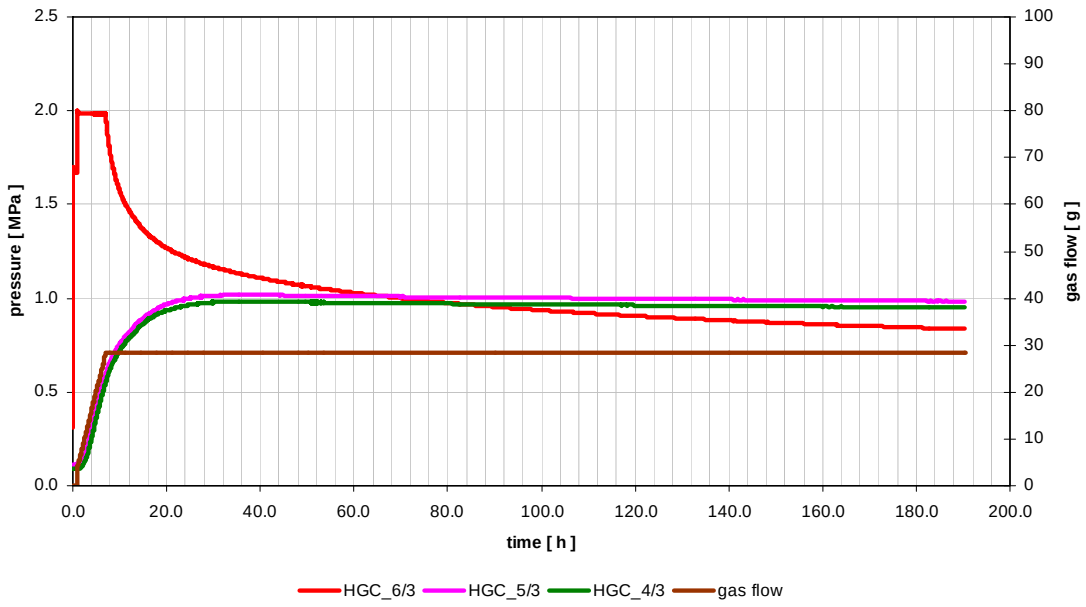

Fig. 5.15 Second injection test at interval BHG-C6/3 (223 days after the first one): Gas break-through at 2.0 MPa to BHG-C5/3 and BHG-C4/3

These two injection tests were again evaluated in terms of effective permeability and both yielded a value of $3 \cdot 10^{-20}$ m^2. On the whole, the geometry of injection boreholes perpendicular to the flow plane is better represented by the WELTEST evaluation, and as a consequence, the fit of these measurements is more satisfying (see Fig. 5.16 for an example).

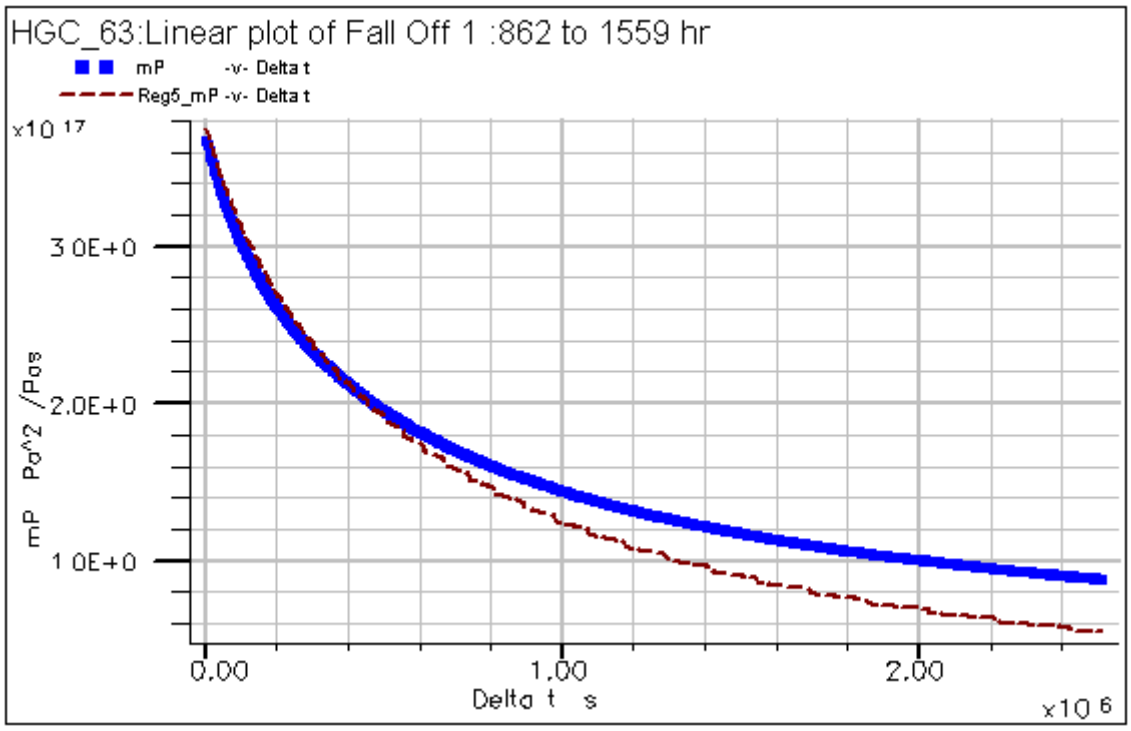

Fig. 5.16 First injection at BHG-C6/3: Measured pressure decay after break-through transformed into pseudo-pressure (blue) and fitted evaluation curve (brown) for an effective permeability of $3 \cdot 10^{-20}$ m^2

Interval BHG-C6/4

This interval was pressurized stepwise up to 3.4 MPa (Fig. 5.17). At the step of 3.2 MPa which lasted for 645.32 hours a small gas flow (2.2 g of nitrogen) was detected. The next pressure step of 3.3 MPa lasted for 506 hours, and 6.2 g of nitrogen flowed. At the pressure step of 33.4 MPa an almost constant flow of $2.8 \cdot 10^{-9}$ m^3s^{-1} was observed for 500 hours. But afterwards the flow rate increased and within the next 335 hours 130 g of nitrogen flowed into the rock, which corresponds to a flow rate of $86 \cdot 10^{-9}$ m^3s^{-1}. Then the gas break through happened and within 18 hours 266 grams of nitrogen flowed into the surrounding rock at a flow rate of $3.28 \cdot 10^{-6}$ m^3s^{-1}. When the gas bottle was empty, the pressure in the injection interval started to decrease.

In contrast to the other injection tests, no pressure increase was detected in any other test interval, meaning there was no connection between the flow path and the other boreholes.

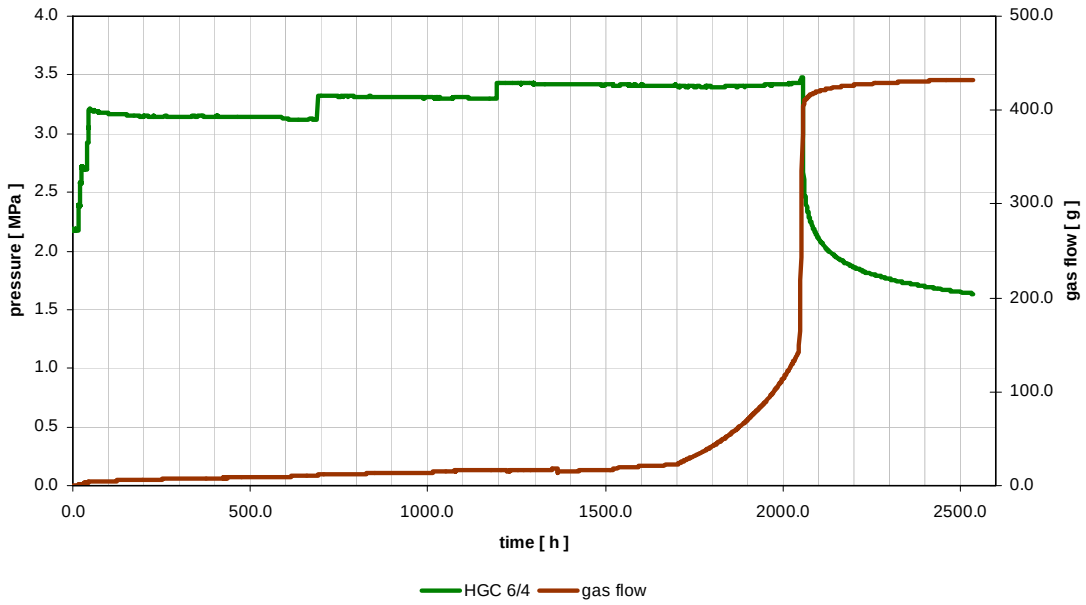

Fig. 5.17 Injection test at interval BHG-C6/4: Gas break-through at 3.4 MPa, no connection to other intervals

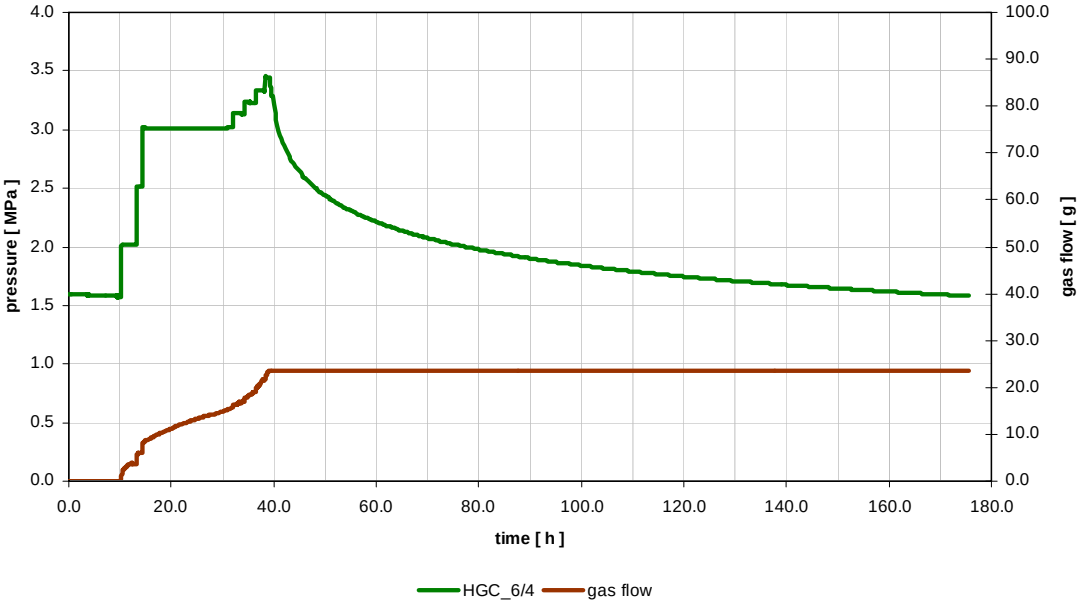

Fig. 5.18 Second injection test at interval BHG-C6/4 (20 days after the first one): No Gas break-through

A second pressure test was also performed at interval BHG-C6/4, 20 days after the first one (Fig. 5.18). This time, no gas break-through was observed at 3.4 MPa, but with increasing injection pressure the flow rate increased. At 3.4 MPa the gas injection was stopped and the interval was sealed. As a result of the gas flow from the interval into

the surrounding host rock the gas pressure decreased in the interval to 1.7 MPa within the next 135 hours. Again, the gas pressure in the other intervals of the boreholes BHG-C4, BHG-C5, and BHG-C6 was not influenced.

The WELTEST evaluation of the test in terms of effective permeability led to a value of $6 \cdot 10^{-21}$ m^2.

6 Summary and Conclusions

Clay formations are proposed as potential host rock for radioactive waste disposal. At the end of the operational phase of the repository the openings, e.g. boreholes, galleries, and chambers have to be backfilled in order to avoid the release of radionuclides into the biosphere. After healing and resaturation of the excavation disturbed zone (EDZ) and saturation of the backfill, the waste containers and the metallic waste components will corrode resulting in the generation of hydrogen. Additionally, carbon dioxide and methane will be released as a result of the oxidation and thermal decomposition of the organic components in the waste and in the clay. If the disposal boreholes and chambers are sealed gas-tight high pressure may be produced leading to the potential generation of fractures in the host rock which could influence the integrity of the repository. For the long-term safety concept of a repository it is therefore essential that the gases migrate through the technical barriers (backfill) and/or into the surrounding host rock at lower pressure and without any irreversible damage of the host rock.

In the Mont Terri underground laboratory in Switzerland gas diffusion and advective gas migration in the Opalinus clay as a function of the gas pressure below the frac pressure were investigated in the frame of the HG-C project. The methods and results are subject of this report.

Different mechanisms of gas migration in clay formations do exist:

- dissolution of the gases in the pore water and diffusion in the liquid phase
- diffusive and advective transport in the gas filled pore volume of the (non saturated) host rock
- two phase gas-water flow in the pore volume of the host rock if the gas entry pressure is exceeded
- dilatancy-controlled gas flow on micro-fracs
- gas flow on macro-fracs

The investigations of the HG-C project were performed in the SB niche which was built in 2004. Two groups of three boreholes with a distance of 50 cm to each other, a diameter of 76 mm, and a length of 10 m were drilled at the wall: Three of the boreholes at the south-east wall with a dip of 40° parallel to the bedding and three of

them at the north-west wall also with a dip of 40° but perpendicular to the bedding. All six boreholes were sealed with quadruple packer systems for gas testing in separate intervals. The data of gas pressure and gas flow were recorded and processed by use of a geomonitor system.

Gas migration in porous media depends on the petrophysical parameters porosity, diffusivity, and permeability, but also on the solution of the gases in the aqueous phase and on the physico-chemical interaction of the gases with the internal surfaces of the different media. In order to determine these effects, tracer gases with different solubilities to water, different sorption behaviours, and different molecular weights were used for the investigations of the migration in the Opalinus clay. The tracer gas mixture consisted of the components 2 vol% hydrogen, helium, neon, krypton, iso-butane, and sulphur hexafluoride each in the matrix of 88 vol% nitrogen.

For investigating the gas migration as a function of the gas pressure three methods were used:

1. Purging an interval with the tracer gas mixture at atmospheric pressure, sealing it for a defined time period and determining the tracer gas concentration decrease after that time period.

2. Pressurizing an interval with the tracer gas mixture to a defined pressure step, sealing it afterwards and determining the pressure and concentration decrease with time.

3. Pressurizing an interval with nitrogen to a defined pressure step, holding that pressure constant and determining the gas flow for holding that pressure constant (constant head test), and recording the pressure decay after stopping the gas flow.

With the results of these investigations and available computer codes the parameters of gas migration as diffusivity and permeability were derived.

The following main results were obtained:

- In the undisturbed region several metres from the niche, the rock is water saturated, and no advective flow occurs below the gas entry pressure. The gas migration mechanism is diffusion of dissolved gas in the liquid phase. For the different tracer gases, effective diffusion coefficients between 10^{-12} and 10^{-10} m^2/s were determined. There is a clear dependence on molecular mass of the tracer.

- Gas entry pressures between 2 and 3.4 MPa were found during constant pressure injection tests. When repeating an injection test, the second entry pressure is somewhat lower. In most cases, gas flow is restricted to the bedding planes. The most probable mechanism at higher pressure is dilatancy controlled gas flow. Effective permeabilities to gas in the range of 10^{-21} to 10^{-19} m^2 were determined.

In order to confirm the results on diffusion coefficients, it would be worthwile to perform a full model calculation of the history of the various successive tracer gas injections. This could not be done in the frame of the HG-C.

The gas migration mechanism at elevated pressure is the focus of the BET project which is still running. The HG-C has provided valuable data that will be further evaluated in the frame of the BET.

7 References

/BOS 03/ Bossart, P., Wermeille, S. (2003): The Stress Field in the Mont Terri Region - Data Compilation. In: Heitzmann, P. & Tripet, J.-P. (ed.): Mont Terri Project – Geology, Palaeohydrology and Stress Field of the Mont Terri Region – Reports of Federal Office for Water and Geology (FOWG), Geology Series 4, 65-92.

/DAN 92/ D'Ans, Lax (1992): Taschenbuch für Chemiker und Physiker, Band 1, Physikalische Daten, Springer Verlag, Berlin.

/JOC 06/ Jockwer, N., H. Kull, K. Wieczorek, R. Miehe (2006): Investigation on Gas Migration, Technical Barriers Concrete and Bentonite as well as Granite of the Surrounding Host rock, Contribution to the Gas Migration Test (GMT) at the Grimsel Test Site, GRS – 221, Gesellschaft für Anlagen- und Reaktorsicherheit (GRS) mbH, ISBN 3-931995-91-7

/JOS 72/ Jost, W., K. Haufe, (1972): Diffusion, Steinkopf Verlag, Darmstadt.

/LID 94/ Lide, D. R. (1994): CRC Handbook of Chemistry and Physiks, 75th Edition, CRC Press, Boca Raton.

/NAG 02-1/ Nagra (2002): Project Opalinus Clay – Safety - Report Demonstration on disposal feasibility for spent fuel, vitrified high-level waste and long-lived intermediate-level waste (Entsorgungsnachweis), Technical report 02-05, Wettingen, Switzerland.

NAG 02-2/ Nagra (2002): Projekt Opalinuston – Synthese der geowissenschaftlichen Untersuchungsergebnisse – Entsorgungsnachweis für abgebrannte Brenn-elemente, verglaste hochaktive sowie langlebige mittelaktive Abfälle. NTB 02-03, Wettingen, Switzerland.

/NEA 04/ OECD (2004): Safety of Disposal of Spent Fuel, HLW and Long-lived ILW in Switzerland, an international peer review of the post-closure radiological safety assessment for disposal in the Opalinus Clay of the Zürcher Weinland, NEA No. 5568.

/NOS 05/ Noseck, U.; Brewitz, W.; Becker, D.A.; Buhmann, D.; Fahrenholz, C.; Fein, E.; Hirsekorn, P.; Keesmann, S.; Kröhn, K.P.; Müller-Lyda, I; Rübel, A.; Schneider, A.; Storck, R. (2005): Wissenschaftliche Grundlagen zum Nachweis der Langzeitsicherheit von Endlagern, GRS-204.

/RÜB 04/ Rübel, A.; Noseck, U.; Müller-Lyda, I.; Kröhn, K.-P.; Storck, R. (2004): Konzeptioneller Umgang mit Gasen im Endlager, GRS-205.

/RÜB 05/ Rübel, A., Buhmann, D., Noseck, U. (2005): Anwendung sicherheits-analytischer Instrumentarien für Endlager in Salz- und Tonformationen. Unterschiede und Gemeinsamkeiten. – Vortrag anlässlich des Workshops GEIST, Peine, 19. und 20.01.2005.

/THU 99/ Thury, M., Bossart, P. (1999): Mont Terri Rock Laboratory – Results of the Hydrogeological, Geochemical and Geotechnical Experiments Performed in 1996 and 1997, Landeshydrologie und –geologie, Geologische Berichte Nr. 23.

/ZHA 07/ Zhang, C.-L., T. Rothfuchs, N. Jockwer, K. Wieczorek, J. Dittrich, J. Müller, L. Hartwig, M. Komischke (2007): Thermal Effects on the Opalinus Clay - A Joint Heating Experiment of ANDRA and GRS at the Mont Terri URL (HE-D Project). Final Report, GRS-224, Gesellschaft für Anlagen- und Reaktorsicherheit (GRS) mbH.

8 List of Figures

9 List of Tables